NASA Technical Memorandum 100455

Flow Visualization Techniques for Flight Research

David F. Fisher and Robert R. Meyer, Jr.

October 1988

National Aeronautics and
Space Administration

NASA Technical Memorandum 100455

Flow Visualization Techniques for Flight Research

David F. Fisher and Robert R. Meyer, Jr.
Ames Research Center, Dryden Flight Research Facility, Edwards, California

1988

National Aeronautics and
Space Administration
Ames Research Center
Dryden Flight Research Facility
Edwards, California 93523-5000

FLOW VISUALIZATION TECHNIQUES FOR FLIGHT RESEARCH

David F. Fisher and Robert R. Meyer, Jr.
NASA Ames Research Center
Dryden Flight Research Facility
P.O. Box 273
Edwards, California 93523-5000
U.S.A.

SUMMARY

In-flight flow visualization techniques used at the Dryden Flight Research Facility of NASA Ames Research Center (Ames-Dryden) and its predecessor organizations are described. Results from flight tests which visualized surface flows using flow cones, tufts, oil flows, liquid crystals, sublimating chemicals, and emitted fluids have been obtained. Off-surface flow visualization of vortical flow has been obtained from natural condensation and two methods using smoke generator systems. Recent results from flight tests at NASA Langley Research Center using a propylene glycol smoker and an infrared imager are also included. Results from photo-chase aircraft, onboard and postflight photography are presented.

NOMENCLATURE

C_p	pressure coefficient
g	load factor normal to longitudinal axis of aircraft
HARV	high alpha research vehicle
h_p	pressure altitude, km (ft)
IR	infrared
LE	leading edge
LEX	leading edge extension
M	Mach number
NLF	natural laminar flow
R	reattachment location
R_n	Reynolds number based on wing reference chord
S_1	primary vortex separation location
S_2	secondary vortex separation location
TACT	transonic aircraft technology
TE	trailing edge
V	velocity
VSFTE	variable sweep flight transition experiment
x/c	ratio of chordwise distance from leading edge to local chord length
α	alpha, angle of attack, deg
δ	boundary layer thickness, cm (in.)
η	ratio of spanwise distance from aircraft centerline to wing semispan
Λ	wing leading edge sweep angle, deg

Subscripts

i	indicated
max	maximum
∞	freestream

1. INTRODUCTION

The visualization of airflow on and about models in wind tunnels has been used for many years to complement other sources of aerodynamic data to help interpret test results. Methods of flow visualization commonly used in wind tunnels include schlieren photography (ref. 1), oil flows (ref. 2), minitufts (ref. 3), vapor screen (refs. 4 and 5), and smoke (ref. 6). From this array of methods, one can choose specific techniques from which shocks can be visualized, flow direction and regions of separated flows can be determined,

boundary layer transition location defined, and vortices identified. Recently, low-speed water tunnels have also been used extensively to visualize simulated airflows (refs. 7 and 8). These techniques and others are well covered in reference 9.

Similarly, a wide variety of in-flight flow visualization techniques for aerodynamic experiments ranging from visualization of boundary layer characteristics to vortical flows have been used at the Dryden Flight Research Facility of NASA Ames Research Center (Ames-Dryden) and its predecessor organizations to help interpret and understand the results of flight tests. These visualization techniques usually give a more global picture of airflow and sometimes are the only way the data can be obtained in flight. Many of the techniques are associated with on-surface flow visualization, including flow cones and tufts, oil flows, a liquid crystal technique, sublimating chemicals, and an emitted fluid technique. Other techniques involve off-surface flow visualization, including two types of smoke generator systems and natural condensation.

The authors discuss the previously mentioned techniques and two other methods used at the NASA Langley Research Center. The reader will be directed to supporting reference material for these in-flight techniques. Verification of the results interpreted from the flow visualization techniques will be made by comparison to other in-flight or ground facility measurements as appropriate.

2. FLOW VISUALIZATION TECHNIQUES

The flow visualization techniques described in the following sections generally require a significant amount of care and fine tuning to get the best results. Ground tests, exploratory flights, or both are usually required to determine the proper viscosity of oil, thickness to apply the liquid crystals, flow rates of emitted fluid, surface color, or proper chemical for sublimation. Flights need to be allocated for development of technique and refinement in the flight planning to ensure favorable results. In addition, careful examination, supporting data, and experience are needed to interpret the results properly.

2.1 Boundary Layer Transition and Shock Visualization Techniques

The techniques that follow are generally used to detect boundary layer transition from laminar to turbulent flow; however, some of the techniques have wider uses. Most of these techniques are dependent upon surface differential temperatures caused by the difference in the laminar and turbulent flow wall recovery factors. Heat sinks such as wing ribs and spars or internal fuel tanks can cause localized cool spots and make these techniques nearly unusable. Smooth insulated fiberglass gloves are generally used for best results.

2.1.1 Oil Flows

Oil flows (refs. 10–13) are obtained by applying an oil mixed with a coloring agent to the surface of an aircraft to study surface flow characteristics. A wide variety of fluid mechanics information can be interpreted from oil flow patterns including location and relative strength of normal shocks, location of boundary layer transition, and identification of areas of separation. These surface flow conditions cause the oil coating to thin, thicken, or puddle, resulting in distinct contrast changes in the oil-coated surface. Various oil viscosities and coloring agents can be blended to provide results at particular flight conditions, such as speed or altitude, or to provide adequate contrast on different colored surfaces.

Results from the oil flow study on the F-111 tactical aircraft technology airplane (TACT)(ref. 12) are presented in figure 1. The study was conducted on a partial span laminar flow glove installed on the left wing panel that was instrumented with a chordwise row of surface static pressure orifices and a boundary layer rake as shown in figure 1(a). For this study, SAE 80-W-90 oil was mixed with powdered black graphite in the proportions of four parts of oil to one part of graphite, by volume. The mixture was applied to the surface with a paint brush approximately 30 min prior to takeoff. Documentation was obtained from chase aircraft photographs.

A dark curved line across the test surface just aft of the midchord can be observed in figure 1(a). This line was attributed to a normal shock wave on the test surface, which causes the oil to build up or puddle,

at the location of the shock. This is verified by the corresponding pressure distribution in figure 1(b). The pressure distribution shows a rapid increase in pressure (more positive C_p) at the same location ($x/c = 0.65$), which also indicates the presence of a shock wave. Meyer and Jennett (ref. 12) showed that the darkness of the line in the oil, indicating a shock, could be correlated directly to relative shock strength as determined from simultaneously obtained pressure distribution data.

A more subtle observation that can be made from oil flows is the location of boundary layer transition from laminar to turbulent flow. An example of this is presented in figure 2 from reference 12. In figure 2(a), note the distinction between a light area forward of the 20-percent chord, where there appears to be little or no oil, and a uniform slightly darkened area aft of the 20-percent chord. The light area is considered to be the region of laminar flow, and the darkened area is considered to be turbulent flow. This interpretation is supported by the corresponding pressure distribution of figure 2(b), as well as the boundary layer data of figure 2(c), from reference 12. In figure 2(b), a favorable pressure gradient exists from the leading edge ($x/c = 0$) to approximately the 20-percent chord ($x/c = 0.20$), where the pressure gradient becomes unfavorable and the boundary layer should transition to a turbulent condition. The variation of upper surface boundary layer thickness, obtained from the boundary layer rakes as a function of angle of attack, is shown in figure 2(c) and described in reference 12. The lines on the figure indicate faired calibration results obtained using "trip strips," and the circular symbol indicates the boundary layer thickness when the oil flow pattern of figure 2(a) was photographed. By referring to the location of the circular symbol with respect to the different calibration lines, the point of transition can be determined, independently of the oil flow, at approximately 23-percent chord ($x/c = 0.23$), confirming the interpretation of the photograph of figure 2(a).

A summary of results using oil flows on seven different aircraft from low speed to supersonic speeds is given in reference 13. Reference 13 also provides details on appropriate oil viscosities and coloring agents for particular applications. With proper flight planning, especially for boundary layer transition location determination, multiple test conditions can be obtained on one flight. Test points with the expected transition location near the leading edge need to be flown before tests points with the transition location far aft. It was also found that this technique was limited to approximately 7600 m (25,000 ft) because the oil becomes too viscous to be of use at the colder temperatures of greater altitudes. Documentation of the oil flow patterns is normally obtained from chase aircraft photographs, although photographs have been obtained in real time from on-board cameras.

2.1.2 Liquid Crystals

Liquid crystals similar to those commonly used in desktop thermometers have been used recently in flight (refs. 14–16) primarily for boundary layer transition visualization. Liquid crystals exposed to fluid flow on the aircraft test surface change color with shear forces or temperatures associated with various fluid mechanic phenomena, such as laminar to turbulent transition or normal shocks.

The liquid crystals are applied to the aircraft by first thinning the liquid crystal solution with solvent and then spraying a very thin coat on the test surface prior to takeoff. The test surface must be a dark color to provide suitable contrast. Holmes and others (ref. 14) reported that a flat black surface provided the best results, although other dark surfaces often provide adequate results. In order to obtain optimum color change with the liquid crystal technique, lighting and viewing angle are critical. Optimum results were obtained with the sun positioned behind the viewer (photo aircraft) and the viewer as close to perpendicular to the test surface as possible.

Results (ref. 16) are presented from the F-14 variable sweep flight transition experiment (VSFTE) program. For those tests, a pressure sensitive liquid crystal (so named by the manufacturer) was applied to laminar flow wing gloves on an F-14 aircraft. The liquid crystals were applied to the surface approximately 1 hr prior to takeoff. Documentation was obtained by photographs and video from a photo chase aircraft.

Examples of liquid crystal patterns on the F-14 airplane's left wing glove are shown in figure 3. Transition is indicated by an abrupt change in color of the liquid crystal pattern due to the discontinuous change in temperature and shear at boundary layer transition. The colors themselves are not important, since they change with viewing angle as well as ambient temperature (altitude).

Figure 3(a) represents a case where transition occurred forward on the test section, probably due to cross-flow disturbance generated by leading edge sweep and is indicated by the sawtooth pattern at approximately 5- to 10-percent chord. Figure 3(b) represents a case where transition occurred about midchord, due to the laminar boundary layer encountering an adverse pressure gradient and is indicated by a uniform line at about 30-percent chord. One other observation in figure 3(b) is the presence of a "transition wedge" near the outboard edge of the test section, probably due to an insect impact or dust stuck in the oily liquid crystal mixture.

Liquid crystal and hot-film transition data obtained at the same time intervals are compared in figure 4 from reference 16. The figure shows that transition location indicated by the liquid crystal flow patterns and hot film agreed to within less than 5-percent chord.

A concern using liquid crystals was the effect, if any, the liquid crystal solution on the test surface might have on the laminar to turbulent boundary layer transition, or in other words, the possibility that the liquid crystal solution would affect or bias the fluid mechanic process. Transition data obtained from the hot films with and without the liquid crystal solution on the test surface are compared in figure 5. Transition is plotted as a function of angle of attack at two representative altitudes. At the lower altitude (higher unit Reynolds number), a variation in transition location of up to 30-percent chord is evident. At the higher altitude (lower unit Reynolds number), there is much less difference, only about 5 percent of chord.

2.1.3 Infrared Imaging

Infrared (IR) imaging is a relatively new flow visualization technique, recently used for nonintrusive visualizing of laminar to turbulent boundary layer transition (refs. 17 and 18). Flight tests with an IR imager were recently conducted at NASA Langley Research Center on a T-34C aircraft modified with an NLF(1)-215F airfoil partial span glove (ref. 18). The sensitivity of the IR imager used in these tests is shown in figure 6. As the temperature of the target surface is increased, the imager becomes more sensitive, so that at 30°C (86°F), the imager can detect differential temperatures of 0.1°C (0.18°F).

The IR camera and display unit were mounted in the T-34C aircraft (fig. 7) with the wing glove in the field of view. The flight tests were conducted with the canopy open so that no loss of image sensitivity occurred from the infrared absorption by the Plexiglas window. During the research flights, an experimenter in the aft cockpit adjusted the imager so that temperature differences on the glove could be observed.

An example of typical results obtained from the IR imager on the black surface during daylight is shown in figure 8. The IR photograph shows that the laminar region (light color) is warmer than the turbulent region. This result is due to the increased convection coefficient of the turbulent boundary layer. The free-stream air temperature is lower than the natural laminar flow (NLF) glove surface due to solar heating, and the turbulent flow region is cooled at a faster rate than the laminar region.

On night flights, the surface temperatures of the NLF glove were much lower because there was no solar radiation effect. Due to the lower temperatures, the sensitivity of the imager was reduced as mentioned previously. As a result, the steady-state level flight test techniques used at night were unsuccessful at low speed. Transition data could be obtained by cold soaking the glove at high altitude, then descending into warmer air so that convection tended to heat the wing as the aircraft descended. Using this technique, the color patterns on the IR images are reversed from that seen during day flights. In figure 9, the laminar areas are dark and the turbulent areas are light.

2.1.4 Sublimating Chemicals

The sublimating chemical technique (refs. 19–21) is used primarily for laminar to turbulent boundary layer transition. The greater heat transfer in the turbulent boundary layer results in higher surface temperatures than in the laminar boundary layer. This elevated temperature and shear associated with turbulence of the boundary layer at the location of transition cause a suitable chemical to increase its rate of sublimation in the turbulent region with respect to that of the laminar region. Consequently, the chemical is removed in the turbulent area before the chemical in the laminar area is appreciably affected.

The chemicals are applied to an aircraft surface by dissolving them in a solvent and then spraying to an appropriate thickness. The solvent evaporates, leaving a crystal structure that can be smoothed if necessary prior to takeoff. The chemicals are white and provide the best contrast on dark surfaces, although dyes, such as food coloring, can be added to the chemicals to provide contrast on light surfaces. Reference 20 contains an excellent summary of various chemicals and application techniques at high speeds and reference 21 summarizes the technique for low speeds. Both sources contain tables and figures that can be used as an aid in choosing particular chemicals for specific applications.

The test aircraft is normally established at the desired test conditions as quickly as possible and then maintains those conditions until the chemicals in the turbulent region have sublimated, showing the desired flow patterns. Normally, the test is documented with photographs taken on the ground, postflight, although photographs can be taken in real time from a chase aircraft or on-board cameras. Unlike the previously described methods, only one flow condition or test point can be obtained per flight.

An example of this technique conducted at speeds near Mach 1.8 on the left wing of an F-104 (ref. 20), using phenanthrene, is shown in figure 10. The aluminum wing was painted black for best contrast with the white chemicals. The transition location was observable as shown in the figure. Note that some of the sublimable chemical along the wing-fuselage juncture and in the rear portion of the wing did not sublimate. This is caused by large structural members that act as heat sinks, thus preventing the wing skin from attaining temperatures high enough to cause a high rate of sublimation.

Another example, this time from the right-hand wing of the F-104 at Mach 2 (ref. 20), is given in figure 11. The right wingtip panel of the F-104 was covered with a thin fiberglass glove, and fluorene was used as the sublimating agent. The test conditions required up to 4 min for the indication of boundary layer transition to be complete. Resistive thermometers can be seen in the photograph (fig. 11) of the wing imbedded beneath the fiberglass and gave good correlation with the sublimation technique.

2.2 Flow Direction and Boundary Layer Separation Visualization Techniques

2.2.1 Flow Cones and Tufts

Tufts, usually made of nylon or wool, have been successfully used in many studies (ref. 22) and are considered a standard method for in-flight flow visualization of surface flow direction and indicators of separation. Flow cones (refs. 23 and 24) were developed to overcome some disadvantages of tufts, such as instability or whipping of tufts (not always related to any feature of the flow) and difficulties in photographing tufts at distances between the photo aircraft and test or research aircraft.

Flow cones are rigid, narrow, hollow conical shapes, attached to an aircraft surface with a short string or chain at the apex of the cone. Like tufts, they are lightweight and align themselves with the local surface flow if the local dynamic pressure is sufficient. A typical tuft and flow cone are compared in figure 12. The flow cones are available in a variety of materials and colors. Photographs are usually taken from a chase aircraft to document the flow cone patterns in flight, however, in some cases, photographs are taken from cameras onboard the test or research aircraft. The flow cones are usually more visible than the tufts since they are larger in diameter and can be covered with reflective material. Though lightweight, their weight (0.7–0.9 gram) can be a disadvantage particularly on the lower surface of wings at low dynamic pressure. In addition, they would not be acceptable in front of engine inlets, whereas, wool tufts probably would be acceptable.

Flow cones and nylon tufts were used recently on the upper surface of left wing and canard of the X-29A aircraft. In figure 13, a comparison of the contrast of a tuft and a flow cone on the X-29A airplane can be seen. These particular photographs represent a slow flight condition for the X-29A aircraft. It was particularly difficult for the photo chase aircraft to photograph at close distance to the test aircraft. Representative tuft and flow cones are identified in the figure. As can be seen in figure 13, the flow cones provided significantly improved contrast and resolution as compared to the tufts.

As a verification of the ability of tufts or flow cones to indicate areas of separated flow, figure 14 shows wing and canard surface static pressure distributions corresponding to the conditions shown in figure 13.

Separated flow in the pressure distributions is indicated by failure of the upper and lower surface pressures to return to a common level at the trailing edge. These trends are evident in the wing upper surface pressure distribution (fig. 14(a)), near midspan ($\eta = 0.49$) on the trailing edge over approximately the aft 10 percent of the wing chord. This interpretation of the wing pressure distributions is consistent with flow cone patterns of figure 13, where the flow cones on the trailing edge are pointed inboard approximately parallel to the trailing edge of the wing. In figure 13, neither the flow cones on the canard nor the pressure distributions of figure 14(b) indicate any flow separation.

2.2.2 Emitted Fluid Technique

Fluids for flow visualization of surface streamlines and areas of separated flow have been used successfully at Douglas Aircraft (refs. 25 and 26), and at Ames-Dryden (ref. 27). This method consists of emitting a small quantity of propylene glycol monomethyl ether (PGME) containing toluene-based dye out of small-diameter surface tubes or orifices on the aircraft skin while the aircraft is stabilized. The flight conditions are held constant for 1–2 min while the fluid evaporates and the dye sets or dries. The dye patterns of the surface streamlines and separated flow regions are documented by photographing the surfaces on the ground after each flight.

An example of surface flow visualization technique on the F-18 forebody for an angle of attack of 30° is shown in the postflight photographs of figure 15. An interpretative cross-sectional flow model (ref. 28) showing the structure of the flow about the forebody for symmetrical flow is illustrated in figure 16. Two primary and two secondary vortices are formed on the leeward side with the separation and reattachment lines noted. As can be seen in figure 15, the remaining dye from this technique clearly showed the surface flow streamlines. Where the streamlines merged, the flow lifted from the surface and rolled up into streamwise vortex cores. Along the streamlines where the flows merge, the separation lines for the vortices were defined. Both the primary and secondary separation lines can be seen. A reattachment line on top of the forebody where the streamlines diverge is also noted.

For both the Douglas and Ames-Dryden tests, a red dye was used with a white painted surface for good contrast. One data point was obtained per flight in this manner. This method is particularly useful when a photo-chase airplane is not available or not practical.

A similar method of using colored ethylene glycol and water on a large commercial transport has been reported (ref. 24). The liquid was emitted from small-diameter tubes distributed upstream of the surface under study. The fluid dispensing cycle took approximately 10 min. The principal data acquisition is air-to-air photography; however, ground inspection of the pattern was also useful to observe and document small details.

2.3 Vortical Flow Visualization Techniques

2.3.1 Natural Condensation Flow Visualization

Flow visualization of vortical flow, expansion, and shock waves, as well as attached and separated flows, can sometimes be observed in flight during periods of high humidity. When the humid air expands around an airplane, it can condense, become visible, and illustrate certain flow patterns such as wing pressure fields, wingtip vortices, and shock waves. A thorough review of this subject with clear examples of the phenomena is given in reference 29. No electromechanical or pyrotechnic devices are needed except the photographic or video recorders.

An example of natural condensation flow visualization on NASA's TACT F-111 aircraft showing the spanwise "gull" pattern over the swept wing and the wingtip vortices is shown in figure 17 (ref. 29). The high velocities and low pressure over the F-111 wing and in the vortices cause the static air temperature to drop and raise the local relative humidity. When the local relative humidity becomes high enough, vapor in the air can condense and become visible.

Similarly, flow visualization in the form of visible vortices due to natural condensation from the leading edge extensions (LEX) on the F-18 high alpha research vehicle (HARV) was noted on some of the initial flights. These vortices (fig. 18) were documented with onboard photography with the flight conditions noted. Note also that after the vortex breaks down, the vortex flow field is no longer visible.

Natural condensation can also occur in flight at supersonic speeds (ref. 29). Vortices can be seen trailing from the canard tips and the outer wing dihedral break of the XB-70 aircraft (fig. 19). Condensation patterns are also visible over the canopy and canard, and a shock pattern can be seen at the trailing edge elevon.

2.3.2 Smoke Generator Systems

Because of the unreliability of natural condensation for flow visualization, smoke generator systems have been developed for visualizing vortical flows in flight (refs. 30–37). Primarily two types of systems have been used, a cartridge system and glycol or oil vaporizer system. Smoke generator systems commonly used at airshows are not applicable for flight research since these systems generally inject oil into the exhaust of the engine and not into the vortex system of interest. For the smoke generator systems used for flight research, smoke is emitted from a duct near the origin of a vortex, allowing the smoke to be entrained in the vortex and permitting a view of the vortex path. Three systems, one cartridge-based system and two vaporizer systems, are discussed as follows.

2.3.2.1 Smoke cartridge systems

Cartridge-based pyrotechnic smoke systems have been used on aircraft to visualize the vortex flow on highly swept wings and leading edge extensions (refs. 30 and 31). Military chemical smoke cartridges were used on the HP115 aircraft (ref. 30) to visualize the vortex on the highly swept wing. A single smoke cartridge and tar trap were mounted externally below the wing near the apex with a duct from the tar trap wrapping around the wing leading edge to the upper surface.

On the NASA F-18 HARV, a smoke generator system (ref. 31) was developed that uses smoke cartridges (fig. 20) designed for this application by the U.S. Army Chemical Research, Development, and Engineering Center, in Aberdeen, Maryland. This system is described in detail in a proposed publication.[1] The smoke cartridges are 6.1 cm (2.4 in.) in diameter and 11.9 cm (4.7 in.) long and were designed to produce nontoxic smoke at a high rate while minimizing fire, detonation or handling hazards. The smoke generator system has been designed into two separate housings, one of which is shown in figure 21. Each housing contains six cartridges and fits within the fuselage of the aircraft. To ensure a safe system, each cartridge is contained within a stainless steel cylinder with a pressure relief to external louvers in the event of high unexpected pressures. The cartridges are temperature controlled at 27°C (80°F) during flight to ensure reliable firing. The six cylinders in each housing are manifolded to a common 2.54 cm (1 in.) diameter duct that exits on either the upper LEX surface near the apex or on the aircraft nosecone. Ducting lengths up to 3 m (9 ft) have been used successfully in flight.

The smoke cartridge system selected for the F-18 aircraft provided a rapid and dense smoke production rate for minimal packaging and power requirements compared to other concepts. Multiple packaging allows from one to six cartridges to be ignited simultaneously, offering a wide range in smoke production rates.

Because the smoke from this system is white, the upper surface of the F-18 HARV was painted a flat black trimmed in gold for good photographic contrast. Four video cameras and one 35 mm camera (fig. 22) were installed on the F-18 airplane to document the results during day flights.

Typical examples of flow visualization of the LEX vortices on the F-18 HARV using the cartridge smoke system are shown in figure 23. As the angle of attack increases, the breakdown location moves forward. An advantage that the smoke has over natural condensation is that the smoke persists beyond the vortex breakdown location.

[1] Proposed NASA Technical Memorandum, *A Smoke Generator System for Aerodynamic Flight Research*, by David M. Richwine, Robert E. Curry, and Gene V. Tracy.

The cartridge smoke system provided visible smoke using two cartridges at a time at speeds from 100 to 140 knots. At speeds up to Mach 0.6, three cartridges were necessary. The cartridges ignited reliably at altitudes as high as 9100 m (30,000 ft). There was a time delay of 10 and 30 sec between ignition and useful smoke production. Once started, a steady stream of useful smoke could be expected for 30 sec when using two or more cartridges. The vortex breakdown data using the F-18 smoke generator system showed close agreement with the natural condensation data. The breakdown location for the LEX vortex as a function of angle of attack (fig. 24) shows good agreement using either natural condensation or smoke techniques. This correlation indicates that the injection of smoke and the external duct did not perturb the flow field significantly to alter the vortex breakdown location.

2.3.2.2 Glycol vaporizers

Researchers at the NASA Langley Research Center have developed a smoke system in which propylene glycol is vaporized into a white smoke with electric heaters on an F-106B aircraft (refs. 32 and 33). Propylene glycol is pumped to the vaporizer containing six 1000-W heaters from an 11.4-L (3 gal) tank onboard the airplane. From the vaporizer, the glycol vapor passes through an insulated and heated pipe to an uninsulated probe tip mounted slightly below the wing near the wing leading edge–fuselage junction. This system provided smoke for approximately 1 hr. The persistence of the propylene glycol smoke from the F-106B during a day flight is shown in figure 25.

This system was usually flown at night with a mercury-arc lamp light sheet system illuminating a nearly perpendicular cut through the vortex core. The light sheet system was mounted in the midfuselage (fig. 26). Documentation was provided by a video camera mounted near the cockpit. While the F-106B aircraft wing was bare aluminum, the authors recommend a flat black paint for improved photographic contrast.

An example of flow visualization using the glycol vaporizer and the light sheet system on the F-106B airplane during a night flight is shown in figure 27(a). The view is from the video camera near the cockpit looking aft at the left wing. The light sheet system illuminates just a slice through the vortices.

The black and white videotape data using the light sheet at night on the F-106B aircraft was enhanced by the image processing laboratory at NASA's Langley Research Center (ref. 33). Examples of the enhanced photos from the same data as figure 27(a) are shown in figure 27(b). In the enhanced photos, the core and flow direction can be readily identified.

2.3.2.3 Corvus oil vaporizers

Corvus oil smoke generators were used by Ames-Dryden in the early 1970s to mark the wake vortices of commercial transports (refs. 34–37). The smoker generators were used from near ground level (2300 ft; 700 m) up to altitudes of 12,500 ft (3800 m). A photograph of the unit mounted on the wing of a B-747 is shown in figure 28.

These units are commercially available in two configurations from Frank Sanders Aircraft, Chino, California. One unit is designed to replace a sidewinder missile while the other fits on the 14-in. NATO bomb rack. The system contains 3.8 L (1.0 gal) of fuel (gasoline) and 38–45 L (10–12 gal) of corvus oil and provides 10–12 min of smoke. Fuel is pumped to a nozzle in a combustor where it is mixed with regulated ram air. A capacitor discharge ignition source charges a coil to fire a spark plug, ignite the fuel–air mixture, and provide heat to vaporize the corvus oil. Oil is pumped to a baffled mixing chamber where it is vaporized and discharged as smoke at the tail of the unit. The system can be cycled on and off. White smoke is obtained using corvus oil, while colored smoke can be obtained by using diesel fuel mixed with dye. The white smoke is the most brilliant. Since the unit burns gasoline and ram air to generate heat, the performance of the system is affected by altitude.

The sidewinder missile configuration is 3.33 m (131 in.) long, 0.184 m (7.25 in.) in diameter, and weighs about 991 kg (200 lb) when full. The bomb rack configuration is 2.04 m (80.5 in.) long, has a diameter of 0.25 m (10 in.), and weighs about 54 kg (120 lb) when full. The system requires 12.5 A of 28 V dc electrical power.

An example of the system in operation on the B-747 is shown in figure 29. Kurkowski and others (ref. 36) note that with the smokers operating at peak performance, the vortex marking smoke could be discerned at approximately 5.6–7.4 km (3–4 n. mi.) behind a B-727 in the landing configuration, allowing intentional vortex penetrations by various probe aircraft.

3. Flow Visualization Recording and Time Correlation

Equally as important to flow visualization as making the flow visible or observing changes in flow indicators is the recording of results. Good photographic or video coverage of the flow visualization having time correlation with the known test conditions is necessary to properly document the results. For example, four video cameras and one 35 mm camera were mounted on the F-18 HARV (fig. 22) to document the visualization of the LEX and forebody vortices. Two of the video signals are telemetered to a ground station for recording and display in real time to a control room. The other two video signals are recorded onboard. The 35 mm camera can be operated by either the pilot or an observer in the ground station to record the results during a test point. A telemetered event mark signal is recorded for each 35 mm photo for time correlation.

Onboard documentation is usually the most effective if the proper viewing angle is available. Chase photos usually do not provide such close time correlation, are difficult to obtain during rapid maneuvers such as wind-up turns, and usually provide poor viewing angles from inside the chase plane canopy.

4. DISCUSSION OF TECHNIQUES

The various in-flight flow visualization techniques are summarized in table 1. The systems are categorized by use, hardware, number of test points per flight and description, and ground or in-flight documentation. The applicable references for each method are also listed.

4.1 Boundary Layer Transition and Shock Visualization Techniques

Four methods of detecting boundary layer transition from laminar to turbulent flow are given. Two of the methods (oil flows and liquid crystals) can also be used to visualize shocks. Except for the sublimating chemical technique, all require in-flight documentation. They are all relatively simple except for IR imaging which requires extensive hardware, including a liquid nitrogen-cooled imager and display. IR imaging is the only nonintrusive method, however. Most of the methods are dependent on the differential temperatures of the laminar and turbulent boundary layers and work best when the surface is insulated from heat sinks, such as with a fiberglass glove. Oil flows are limited to altitudes of approximately 7600 m (25,000 ft), liquid crystals to about 10,700 m (35,000 ft), IR imaging to about 5500 m (18,000 ft), while sublimating chemicals have been used as high as 16,800 m (55,000 ft). The IR imaging limit is for an unpressurized instrumentation compartment, but it could be used at higher altitudes with pressurization and special IR-compatible viewing ports.

Liquid crystals are currently the most widely used method of detecting the laminar to turbulent transition location through flow visualization. These, in general, provide favorable results and are capable of continuously and quickly reacting to flow changes, allowing multiple test points to be obtained per flight. However, several precautions need to be taken when using them. Insects and dust in greater amounts tend to adhere to glove surfaces coated with liquid crystals than on uncoated surfaces, potentially causing premature transition and contaminating test results. Uneven thickness in the liquid crystal coat can cause changes of color of the liquid crystal pattern, interfering with interpretation of the patterns. Also, at high unit Reynolds number, the presence of the liquid crystal coat can move the transition location forward.

4.2 Flow Direction and Boundary Layer Separation Visualization Techniques

Two methods of detecting surface flow direction and boundary layer separation are listed. The flow cone–tuft technique is much simpler than the emitted fluid method and provides multiple test points, but

does require in-flight documentation. The emitted fluid technique is much more complicated, requires stabilized test points of 1–2 min, but can produce good results when in-flight documentation is not available or practical.

For the surface flow visualization methods using oils, liquid crystals, sublimating chemicals, and fluid, the surface needs to be cleaned of all dirt, grease, or oil prior to application. Gaps and joints in the aircraft skin should be sealed or taped. Many of these techniques use solvents and toxic chemicals, so proper clothing and adequate ventilation should be used.

4.3 Vortical Flow Visualization Techniques

Natural condensation flow visualization can be useful, especially in leading researchers to areas of interest, particularly with respect to vortical flows. However, it is difficult to predict when it might occur, especially for flight planning. It is usually advantageous, especially with the study of vortical flows.

Three different types of smoke generator systems are noted for visualizing vortical flows in the absence of natural condensation. All three systems require fairly extensive hardware installations. The cartridge system and the corvus oil vaporizer supply the largest quantities of smoke for relatively short periods, while the glycol vaporizer can provide smoke for up to 1 hr. Both the cartridge system and the glycol vaporizer can be mounted internally and ducted to the exit port. All three methods require that certain precautions be taken to make them safe for flight research.

5. CONCLUDING REMARKS

In-flight flow visualization has been shown to be useful in the understanding of fluid mechanics. It provides a global view of the airflow and is sometimes the only way the data can be obtained. The results of using ten different methods of flow visualization for flight research can be summarized as follows: oil flows, liquid crystals, and sublimating chemicals are useful flow visualization techniques for detecting boundary layer transition from laminar to turbulent flow. Infrared imaging is a new unintrusive technique for detecting transition but requires extensive hardware. Only sublimating chemicals do not require in-flight documentation, however, each flight yields data for only one test condition.

Flow direction and separation can be determined using flow cones, tufts, and the emitted fluid flow visualization techniques. Flow cones and tufts can provide data during dynamic maneuvering, thereby requiring in-flight documentation. Stabilized test conditions from 1– 2 min and extensive hardware are needed for the emitted fluid technique, and only one test condition per flight can be documented.

For visualizing vortex flows, three smoke generator systems are available but all require fairly extensive hardware installations.

Natural condensation is essentially free and can be useful for the flow visualization of vortices and shocks and for leading researchers to areas of interest.

The knowledge of the test flight conditions is nearly as important as the flow visualization itself irrespective of the technique used.

REFERENCES

1. Bracht, K., and W. Merzkirch, "Schlieren Visualization of the Laminar-to-Turbulent Transition in a Shock-Tube Boundary Layer," AIAA A79-12898, Oct. 1977.

2. Loving, Donald L., and S. Katzoff, *The Fluorescent-Oil Film Method and Other Techniques for Boundary-Layer Flow Visualization*, NASA Memo 3-17-59L, Langley Research Center, 1959.

3. Crowder, James P., "Add Fluorescent Minitufts to the Aerodynamicist's Bag of Tricks," *Astronaut. & Aeronaut.*, Nov. 1980.

4. Allen, H. Julian, and Edward W. Perkins, *A Study of Effects of Viscosity on Flow Over Slender Inclined Bodies of Revolution*, NACA Report 1048, 1951.

5. Erickson, G.E., L.W. Rogers, J.A. Schreiner, and D.G. Lee, "Subsonic and Transonic Vortex Aerodynamics of a Generic Chine Forebody-Slender Wing Fighter," AIAA 88-2596, June 1988.

6. Nelson, Robert C., "The Role of Flow Visualization in the Study of High-Angle-of-Attack Aerodynamics," in *Tactical Missile Aerodynamics*, vol. 104, M.J. Hemsch and J.N. Nielson, eds., 1986, pp. 43–88.

7. Erickson, Gary E., David J. Peake, John Del Frate, Andrew M. Skow, and Gerald N. Malcolm, "Water Facilities in Retrospect and Prospect—An Illuminating Tool for Vehicle Design," AGARD CP-413, 1987, pp. 1-1–1-28.

8. Werlé, H. "Possibilites D'Essai Offertes Par Les Tunnels Hydrodynamiques a Visualisation de L'Onera Dans Les Domaines Aeronautique et Naval" ("The Onera Water Tunnels Test Possibilities for Flow Visualization in Aeronautical and Naval Domains"), AGARD CP-413, 1987, pp. 14-1–14-16.

9. Merzkirch, Wolfgang, *Flow Visualization*, 2nd ed., Academic Press, Inc., 1987.

10. Johnson, Harold I., and Robert G. Mungall, *A Preliminary Flight Investigation of an Oil-Flow Technique for Air-Flow Visualization*, NACA RM L54G14a, 1954.

11. Bisgood, P. L., The Application of a Surface Flow-Visualization Technique in Flight, A.R.C. R&M 3769, 1974.

12. Meyer, Robert R., Jr., and Lisa A. Jennett, *In-Flight Surface Oil-Flow Photographs With Comparisons to Pressure Distribution and Boundary-Layer Data*, NASA TP-2395, 1985.

13. Curry, Robert E., Robert R. Meyer, Jr., and Maureen O'Connor, *The Use of Oil for In-Flight Flow Visualization*, NASA TM-84915, 1983 (rev. 1984).

14. Holmes, Bruce J., Peter D. Gall, Cynthia C. Croom, Gregory S. Manuel, and Warren C. Kelliher, *A New Method for Laminar Boundary Layer Transition Visualization in Flight—Color Changes in Liquid Crystal Coatings*, NASA TM-87666, 1986.

15. Holmes, Bruce J., and Clifford J. Obara, "Advances in Flow Visualization Using Liquid-Crystal Coatings," SAE Paper 871017, 1987.

16. Anderson, Bianca Trujillo, Robert R. Meyer, Jr., and Harry R. Chiles, "Techniques Used in the F-14 Variable-Sweep Transition Flight Experiment," AIAA 88-2110, May 1988.

17. Körner, H., K.H. Horstmann, H. Köster, A. Quast, and G. Redeker, "Laminarization of Transport Aircraft Wings—A German View," AIAA 87-0085, Jan. 1987.

18. Brandon, J.M., G.S. Manuel, R.E. Wright, and B.J. Holmes, "In-Flight Flow Visualization Using Infrared Imaging," AIAA 88-2111, May 1988.

19. Banner, Richard D., John G. McTigue, and Gilbert Petty, Jr., *Boundary-Layer-Transition Measurements in Full-Scale Flight*, NACA RM-H58E28, 1958.

20. McTigue, John G., John D. Overton, and Gilbert Petty, Jr., *Two Techniques for Detecting Boundary-Layer Transition in Flight at Supersonic Speeds and at Altitudes Above 20,000 Feet*, NASA TN D-18, 1959.

21. Obara, Clifford J., "Sublimating Chemical Technique for Boundary-Layer Flow Visualization in Flight Testing," *J. Aircraft*, vol. 25, no. 6, June 1988. Also available as AIAA 85-2413 and NASA CP-2413, pp. 129–140, Apr. 1985.

22. Montoya, Lawrence C., Paul F. Bikle, and Richard D. Banner, "Section Drag Coefficients From Pressure Probe Traverses of a Wing Wake at Low Speeds," NASA CP-2045, part 2, pp. 601–621, 1978.

23. Crowder, James P., and Paul E. Robertson, "Flow Cones for Airplane Flight Test Flow Visualization," in *Flow Visualization III*, W. J. Yang, ed., Hemisphere Publ. Corp., 1985, pp. 60–64.

24. Crowder, James P., "Flow Visualization Techniques Applied to Full-Scale Vehicles," AIAA 87-2421, 1987.

25. Belevtsov, N., R.E. Brumby, and J.P. Hughes, "In-Flight Flow Visualization, a Fluid Approach," Society of Flight Test Engineers, 14th Annual Symposium Proceedings, Aug. 1983, pp. 4.2-1–4.2-7.

26. Hughes, J.P., R.E. Brumby, and N. Belevtsov, "Flow Visualization From the Ground Up," AIAA 83-2691, Nov. 1983.

27. Fisher, David F., David M. Richwine, and Daniel W. Banks, *Surface Flow Visualization of Separated Flow on the Forebody of an F-18 Aircraft and Wind-Tunnel Model*, NASA TM-100436, 1988.

28. Peake, D.J, D.F. Fisher, and D.S. McRae, "Flight, Wind Tunnel, and Numerical Experiments With a Slender Cone at Incidence," *AIAA Journ.*, vol. 20, no. 10, Oct. 1982, pp. 1338–1345.

29. Campbell, James F., Joseph R. Chambers, and Christopher L. Rumsey, "Observation of Airplane Flow Fields by Natural Condensation Effects," AIAA 88-0191, Jan. 1988.

30. Fennell, L.J., *Vortex Breakdown—Some Observations in Flight on the HP115 Aircraft*, Reports and Memoranda No. 3805, Sept. 1971 (replaces R.A.E. Technical Report 71177, A.R.C. 34 400).

31. Curry, Robert E., and David M. Richwine, "An Airborne System for Vortex Flow Visualization on the F-18 High-Alpha Research Vehicle," AIAA 88-4671, Sept. 1988.

32. Lamar, John E., Philip W. Brown, Robert A. Bruce, Joseph D. Pride, Jr., Ronald H. Smith, and Thomas D. Johnson, Jr., *Operational Performance of Vapor-Screen Systems for In-Flight Visualization of Leading-Edge Vortices on the F-106B Aircraft*, NASA TM-4004, 1987.

33. Lamar, John E., and Thomas D. Johnson, Jr., *Sensitivity of F-106B Leading-Edge-Vortex Images to Flight and Vapor-Screen Parameters*, NASA TP-2818, 1988.

34. Tymczyszyn, Joseph J., and Marvin R. Barber, "Recent Wake Turbulence Flight Test Programs," 1974 Report to the Aerospace Profession—Eighteenth Symposium Proceedings, Soc. Experimental Test Pilots, vol. 12, no. 2, Sept. 1974, pp. 52–68.

35. Jacobsen, Robert A., and M.R. Barber, "Flight-Test Techniques for Wake-Vortex Minimization Studies," NASA SP-409, 1976, pp. 193–219.

36. Kurkowski, R.L., M.R. Barber, and L.J. Garodz, *Characteristics of Wake Vortex Generated by a Boeing 727 Jet Transport During Two-Segment and Normal ILS Approach Flight Paths*, NASA TN D-8222, April 1976.

37. Smith, Harriet J., *A Flight Test Investigation of the Rolling Moments Induced on a T-37B Airplane in the Wake of a B-747 Airplane*, NASA TM X-56031, 1975.

6. ACKNOWLEDGMENTS

The authors wish to thank Dr. John Lamar and Jay Brandon of NASA Langley Research Center for material on glycol vaporizers and infrared imaging, respectively, provided for this paper. Thanks are also due to Lisa Jennett Bjarke, Edwin Saltzman, Robert Curry, Bianca Trujillo Anderson, David Richwine, and John Del Frate of NASA Ames-Dryden for their assistance and contributions to this paper.

TABLE 1. SUMMARY OF FLOW VISUALIZATION TECHNIQUES

Technique	Primary use	Hardware	Test points–flight	Test point description	Documentation	References
Oil flows	Transition location, shock location	Simple	Multiple	Stabilized	In flight	10–13
Liquid crystals	Transition location, shock location	Simple	Multiple	Stabilized	In flight	14–16
Infrared imaging	Transition location	Extensive	Multiple	Stabilized	In flight	17–18
Sublimating chemicals	Transition location	Simple	Single	Stabilized up to 4 min	Postflight, in flight	19–21
Flow cones–tufts	Flow direction, separation	Simple	Multiple	Dynamic	In flight	22–24
Emitted fluid	Flow direction, separation	Extensive	Single	Stabilized 1–2 min	Postflight, in flight	24–27
Natural condensation	Vortical flow definition	None	Multiple	Dynamic	In flight	29
Smoke Systems						
Cartridge	Vortical flow definition	Extensive	Multiple	Dynamic, ~ 30 sec	In flight	30–31
Glycol vaporizers	Vortical flow definition	Extensive	Multiple	Dynamic, up to 1 hr	In flight	32–33
Corvus oil vaporizers	Vortical flow definition	Moderate	Multiple	Dynamic, up to 12 min	In flight	34–37

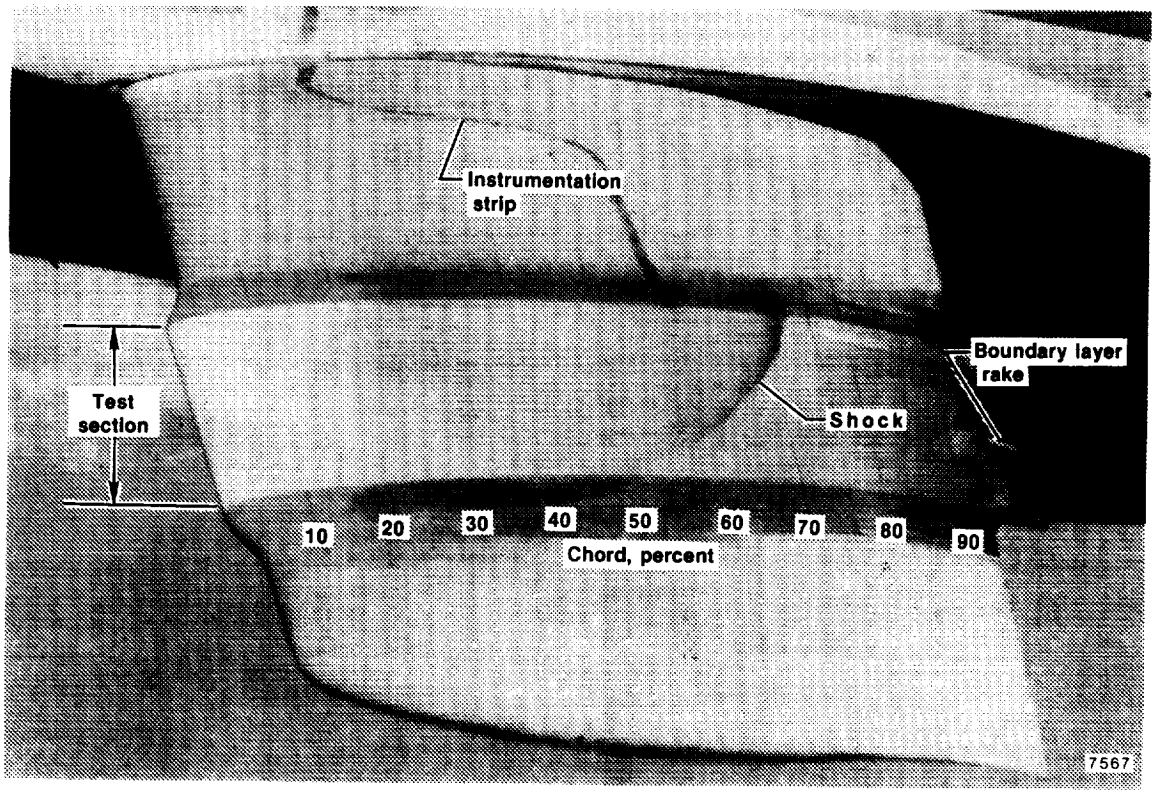

ECN 13418

(a) Glove test section with oil.

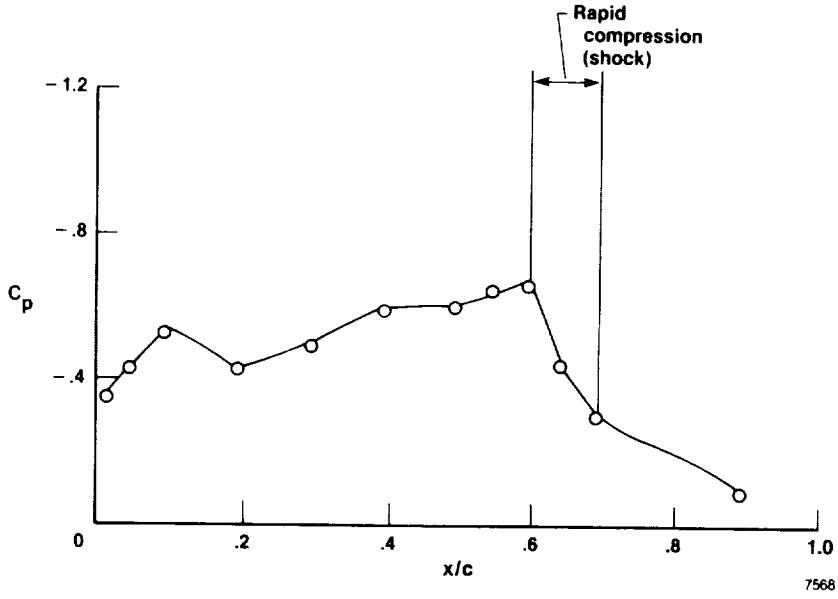

(b) Pressure distribution for glove test section with oil.

Figure 1. F-111 TACT glove test section upper surface oil flow photograph and pressure distribution, $M = 0.85$, $\alpha = 4.7°$, and $\Lambda = 25°$.

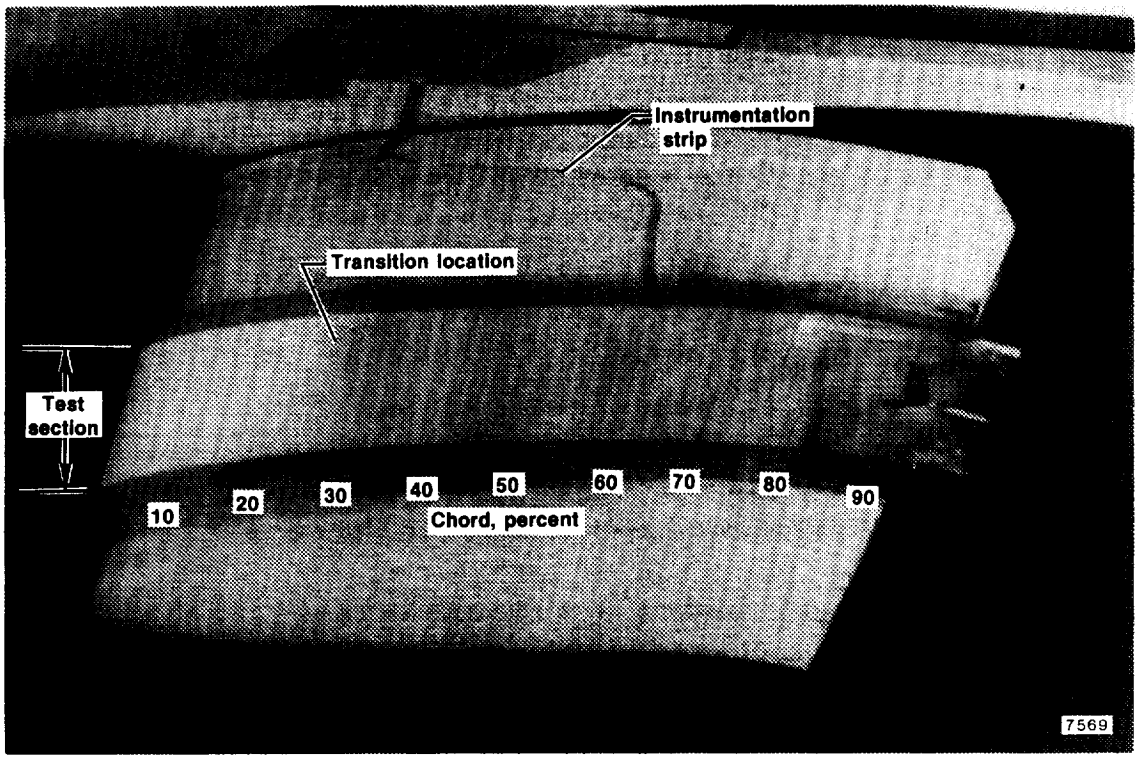

ECN13419

(a) Glove test section with oil.

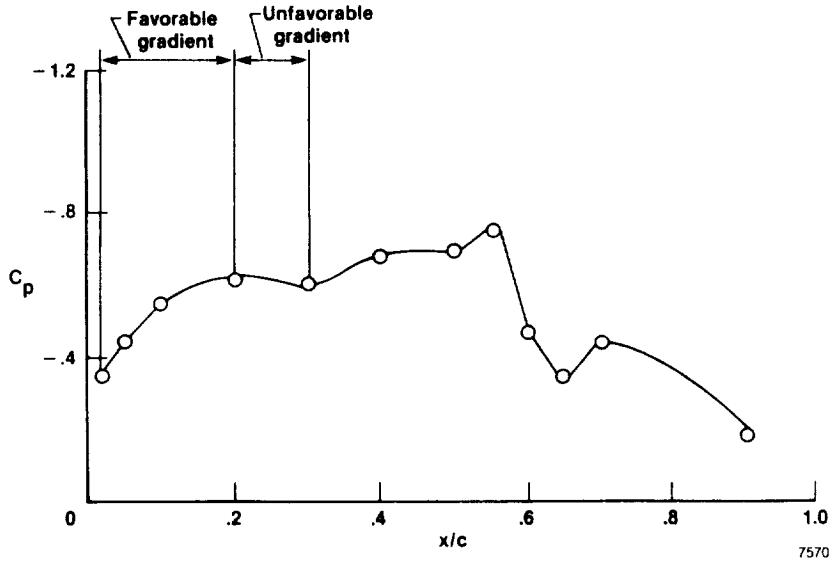

(b) Pressure distribution for glove test section with oil.

Figure 2. F-111 TACT test section upper surface oil flow photograph, pressure distribution, and boundary layer thickness, $M = 0.83$, $\alpha = 4.9°$, and $\Lambda = 16°$.

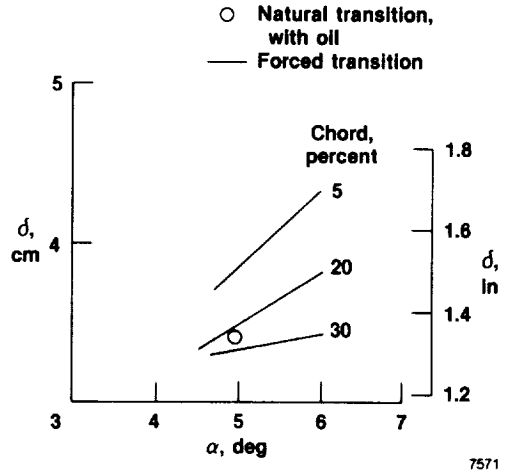

(c) Determination of transition location using forced transition locations.

Figure 2. Concluded.

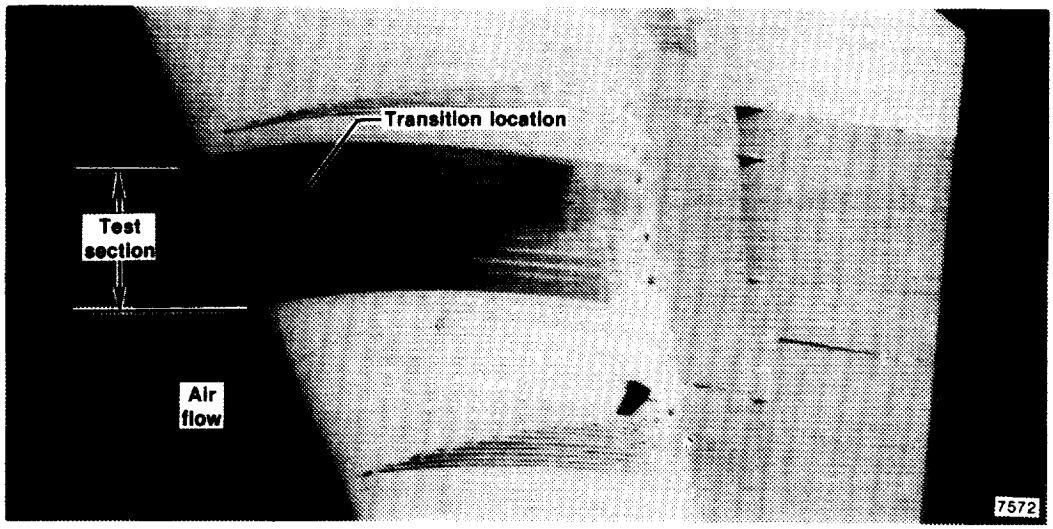

EC 86-33600-018

(a) Sawtooth pattern near wing leading edge.

Figure 3. Examples of liquid crystal patterns.

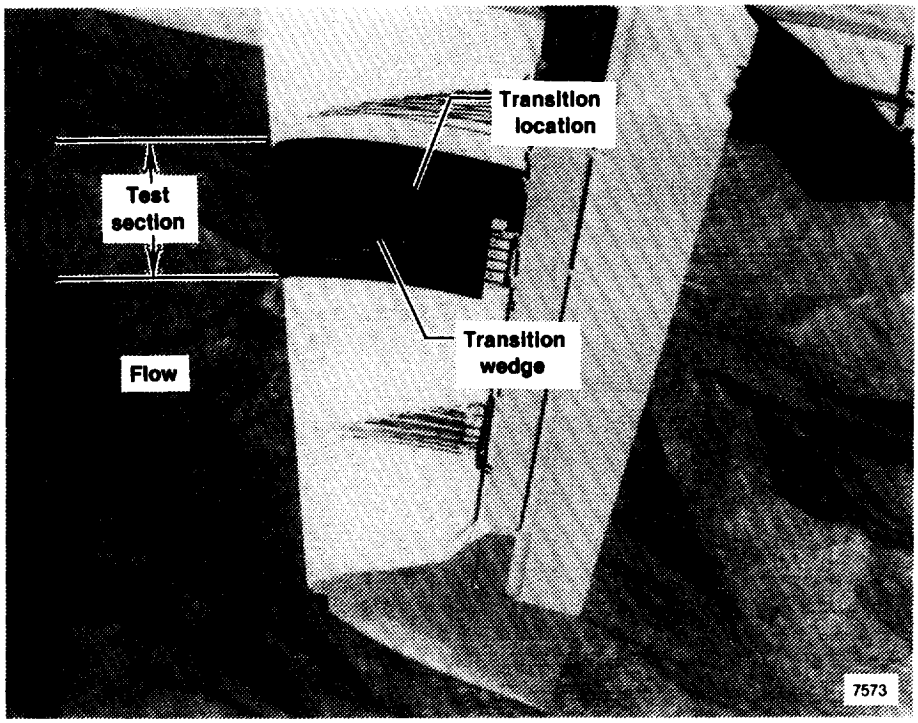

EC 86-33598-016

(b) Uniform line pattern near midchord.

Figure 3. Concluded.

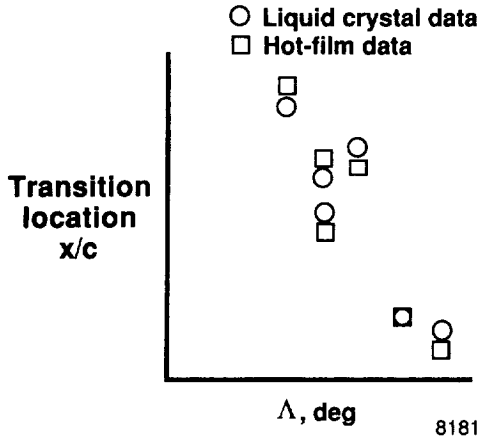

Figure 4. Comparison of transition locations determined by hot-film and liquid crystal techniques.

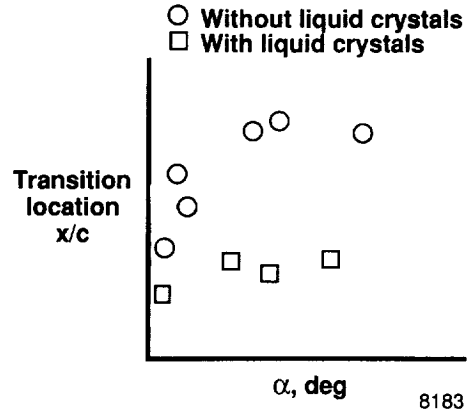

(a) Low-altitude data.

Figure 5. Comparison of transition locations determined by hot-film technique with and without liquid crystals on glove surface.

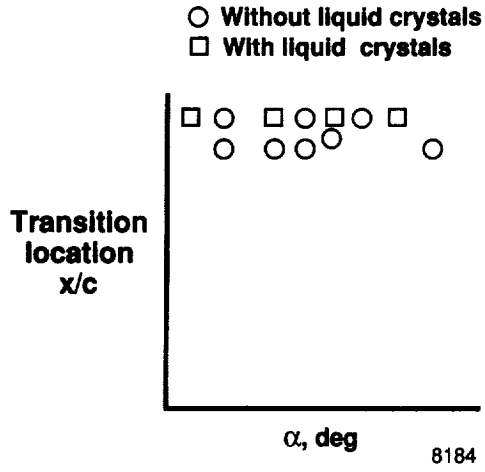

(b) High-altitude data.

Figure 5. Concluded.

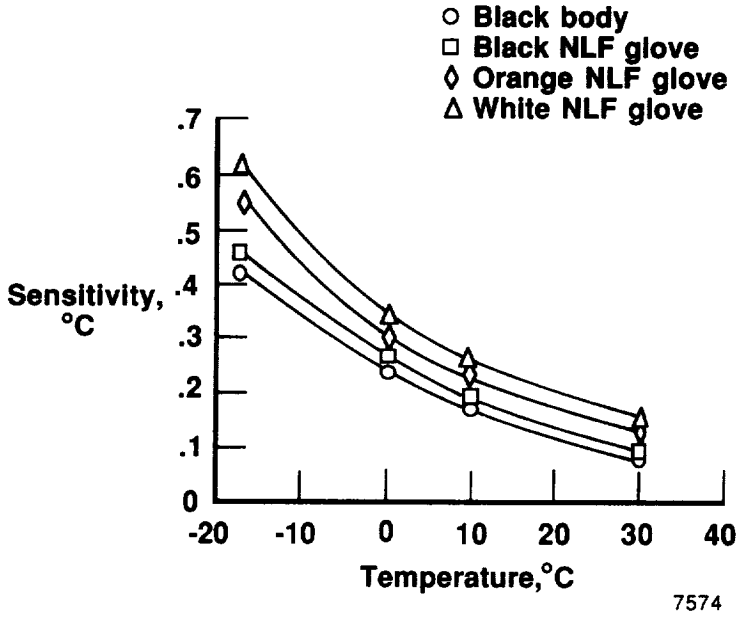

Figure 6. Effect of target temperature on minimum detectable temperature gradient of IR imager.

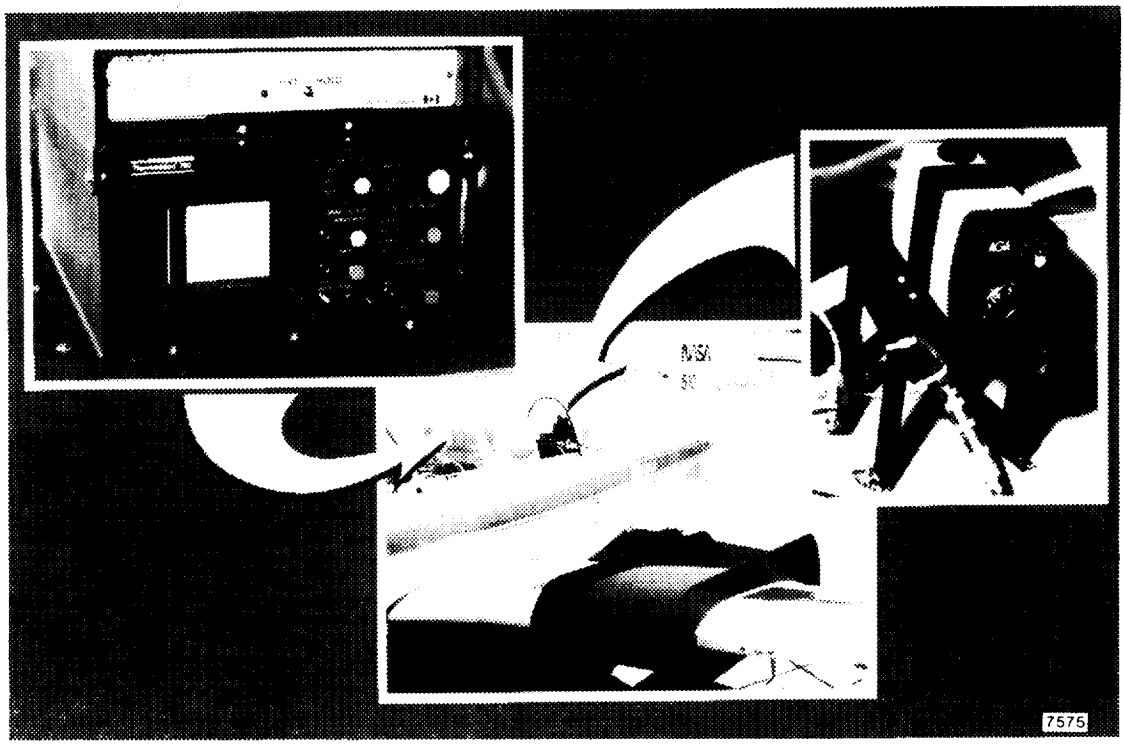

Figure 7. T-34C aircraft and IR imager test setup.

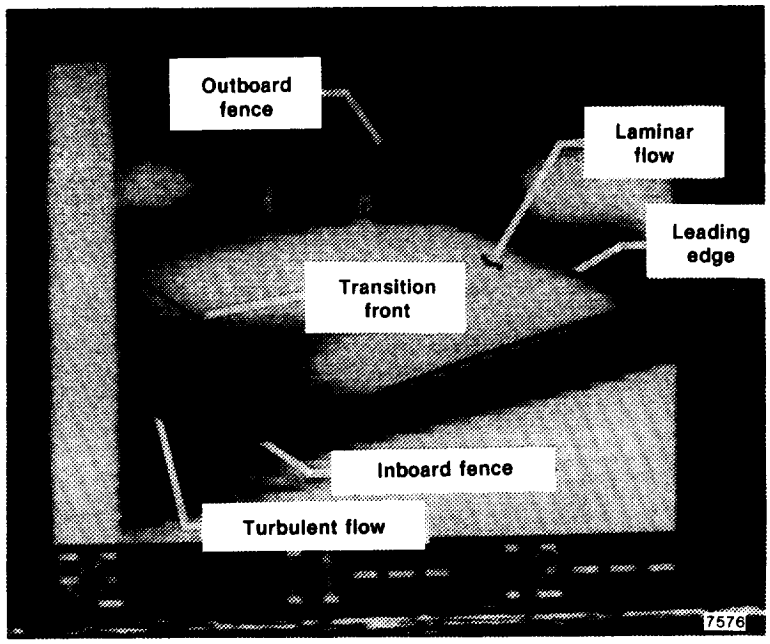

Figure 8. Results of IR imaging from T-34C wing glove during day flight, V_i = 178 knots.

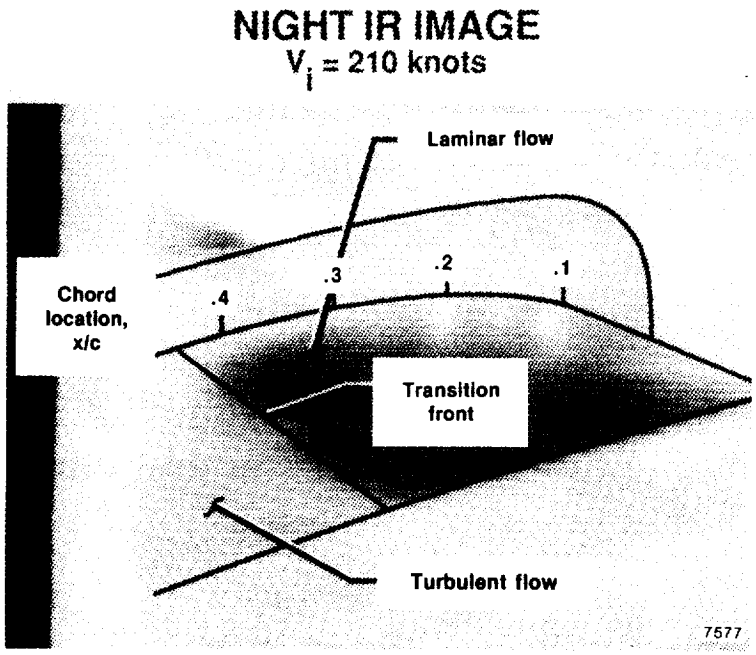

Figure 9. Results of IR imaging from T-34C wing glove during night flight, V_i = 210 knots.

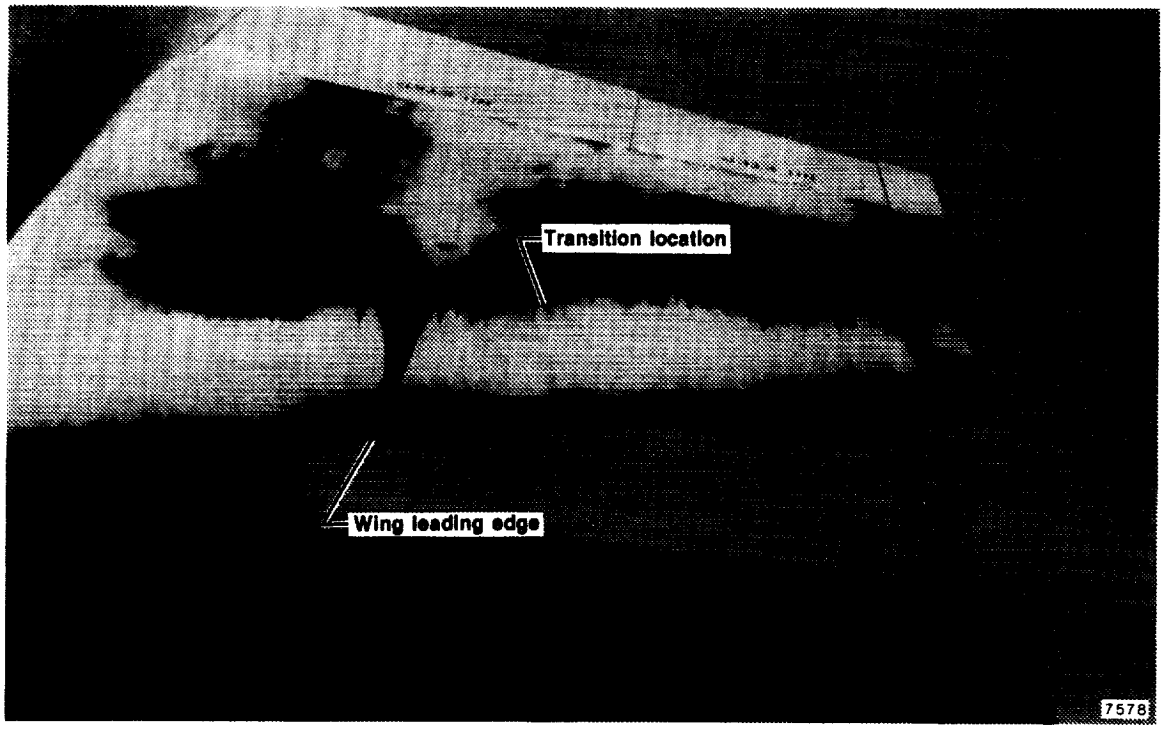

E-3513

Figure 10. Postflight example of sublimating chemical technique on the black painted F-104 left wing, phenanthrene; M_{max} = 1.8, h_p = 16,200 m (53,000 ft).

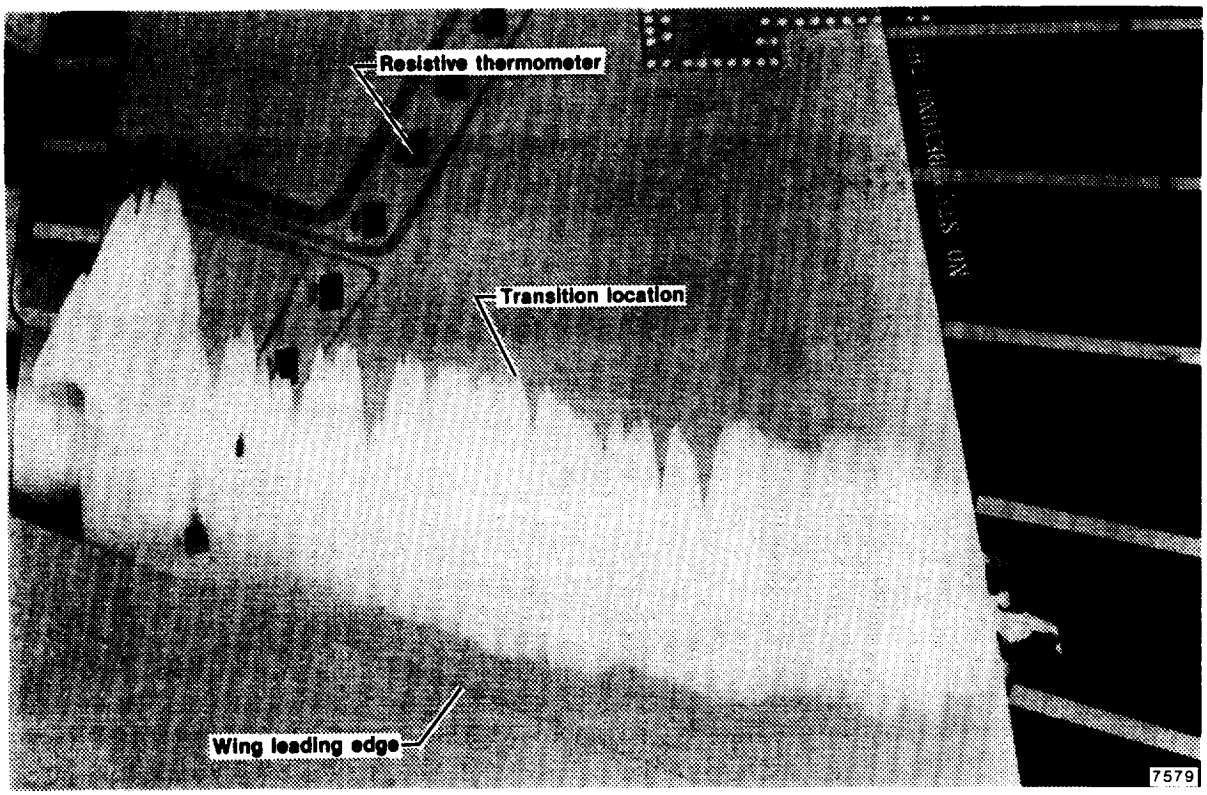

E-3355

Figure 11. Postflight example of sublimating chemical technique on the fiberglass glove F-104 right wing-tip panel, fluorene; $M_{max} = 2.0$, $h_p = 16{,}800$ m (55,000 ft).

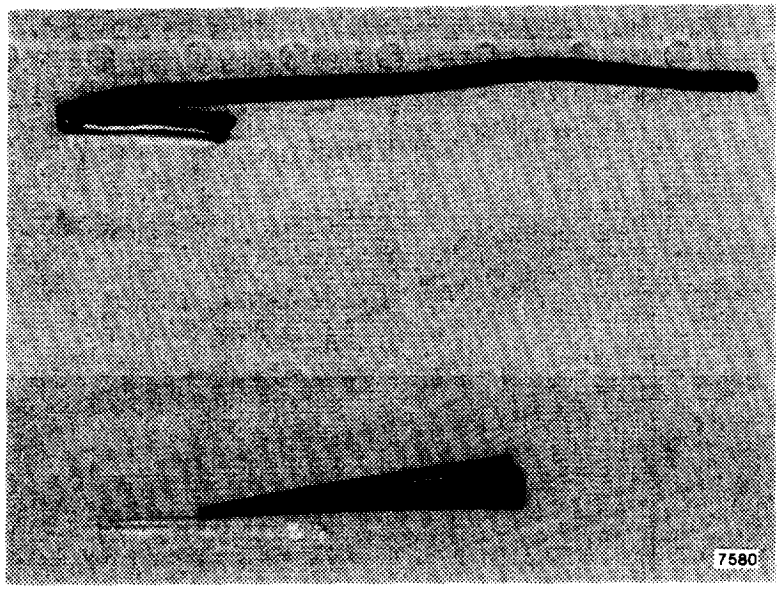

Figure 12. Typical flow cone and tuft.

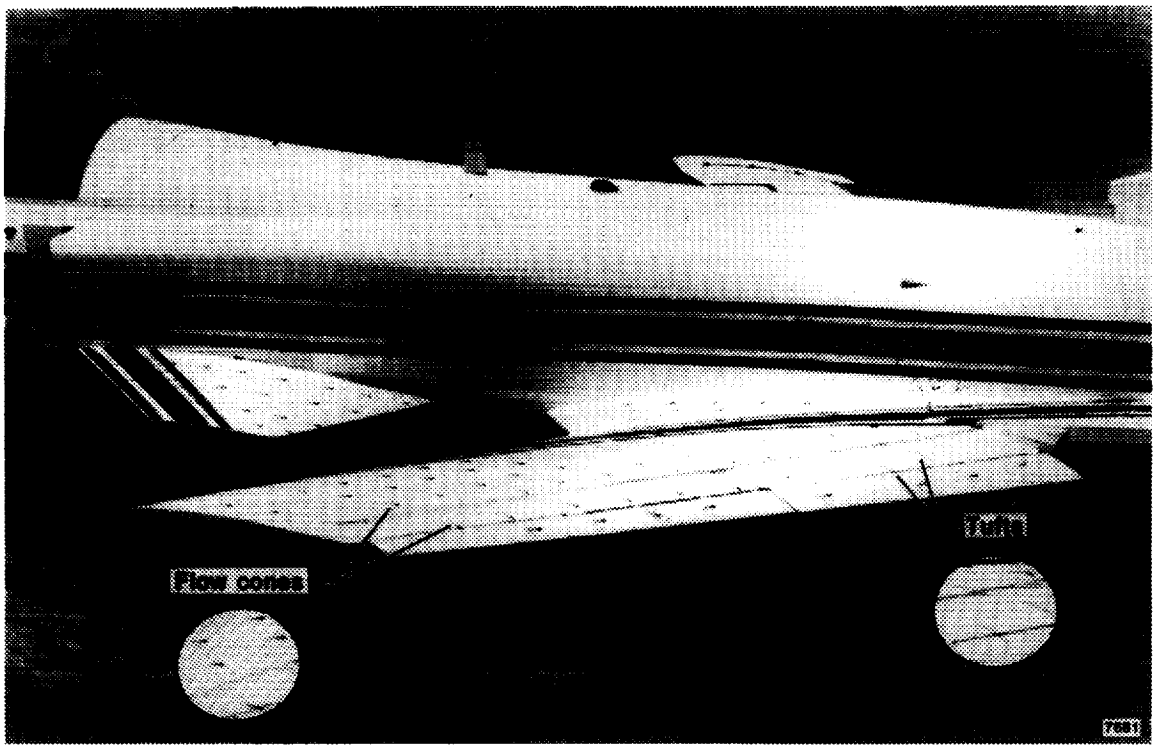

Figure 13. Flow cones and tufts on the left wing and canard of the X-29A aircraft.

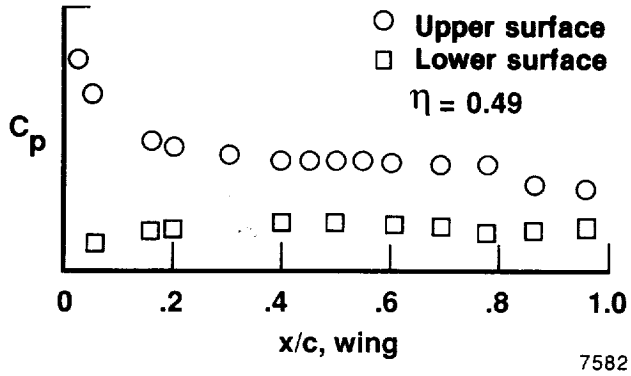

(a) Wing.

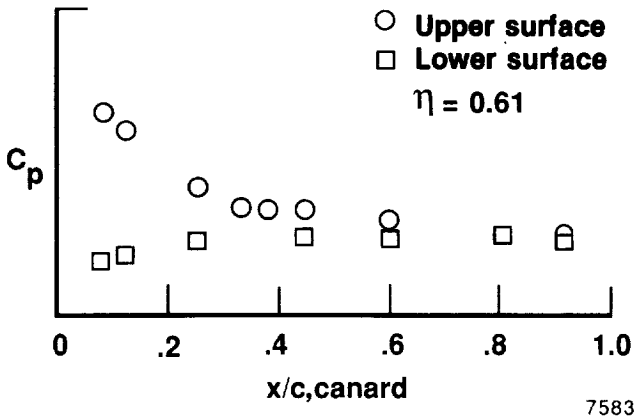

(b) Canard.

Figure 14. X-29A aircraft wing and canard pressure distribution.

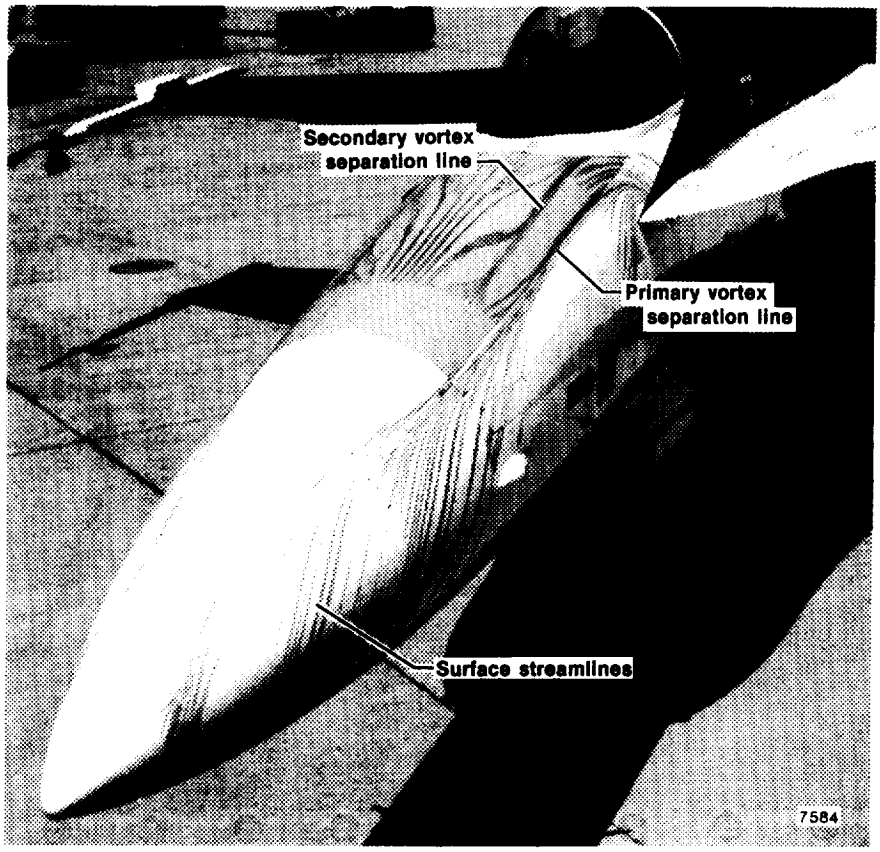

(a) 1/4 view of forebody.

Figure 15. Postflight visualization of surface streamlines and lines of separation on F-18 forebody, $\alpha = 30°$.

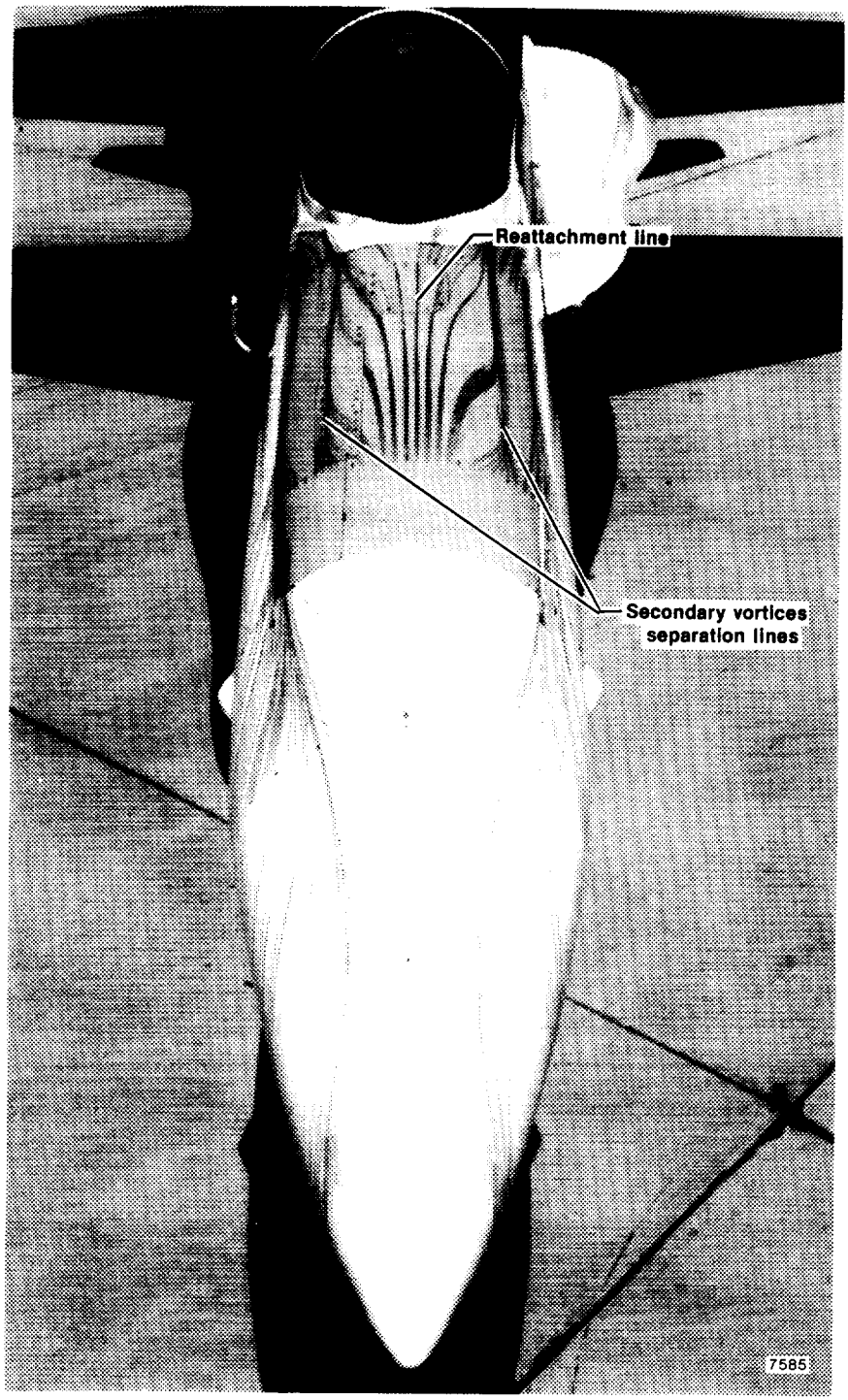

(b) Head-on view of forebody.

Figure 15. Concluded.

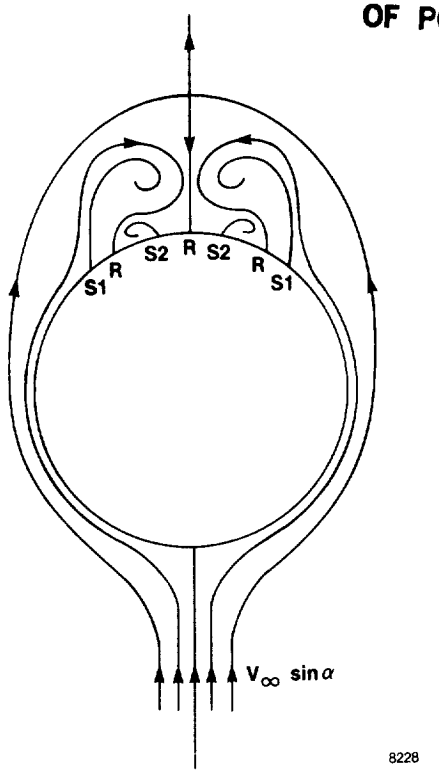

Figure 16. Model of flow about forebody, symmetrical flow (cross-sectional view).

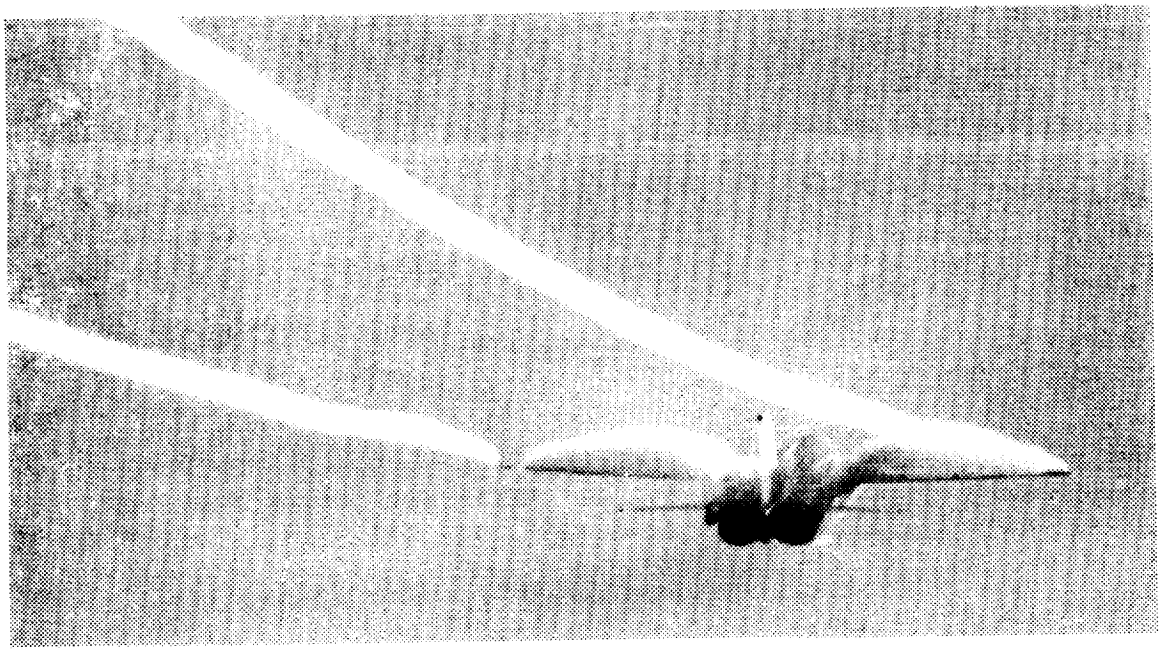

ECN 9514

Figure 17. Wing "gull" pattern and tip vortices on the F-111 TACT aircraft, $M_\infty = 0.82$, $\alpha = 6.9°$, $g = 3.3$.

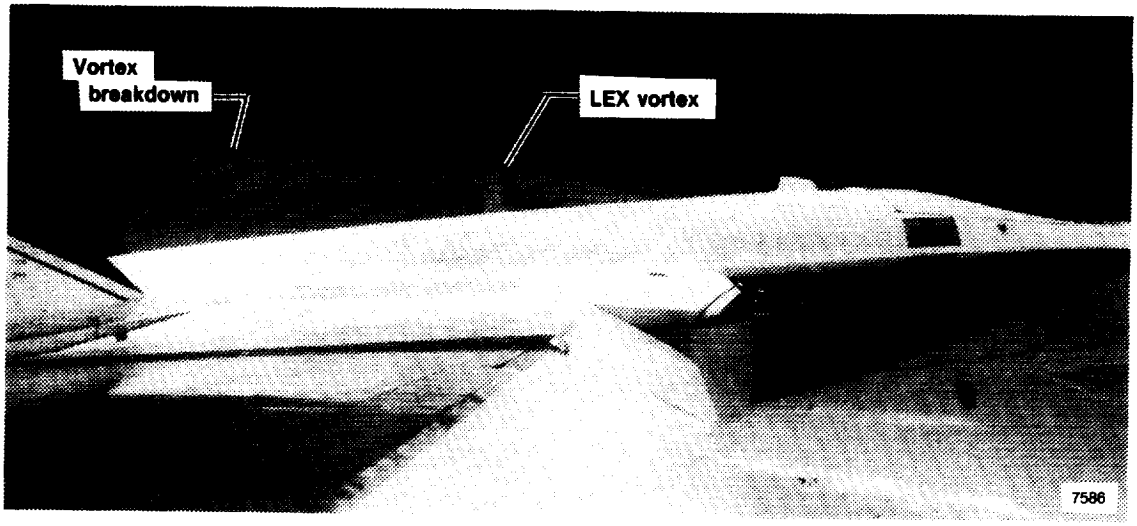

EC 87 0160-026

Figure 18. Natural condensation of LEX vortices on the F-18 HARV aircraft, $\alpha = 19.2°$

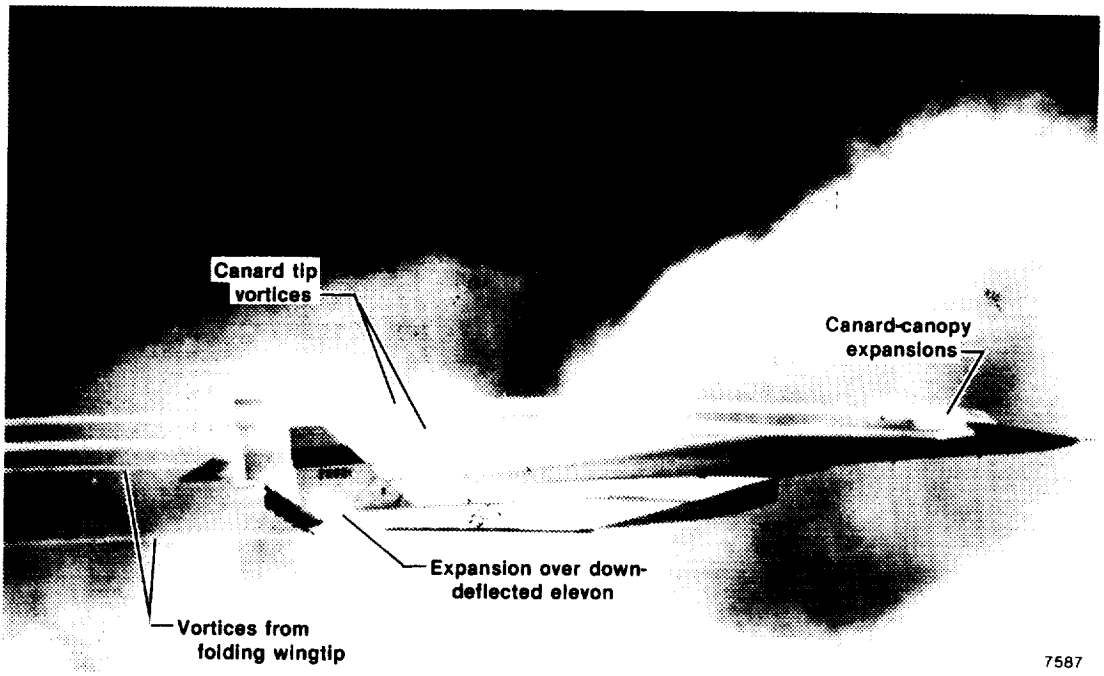

Figure 19. Condensation patterns on the XB-70 aircraft at supersonic speed.

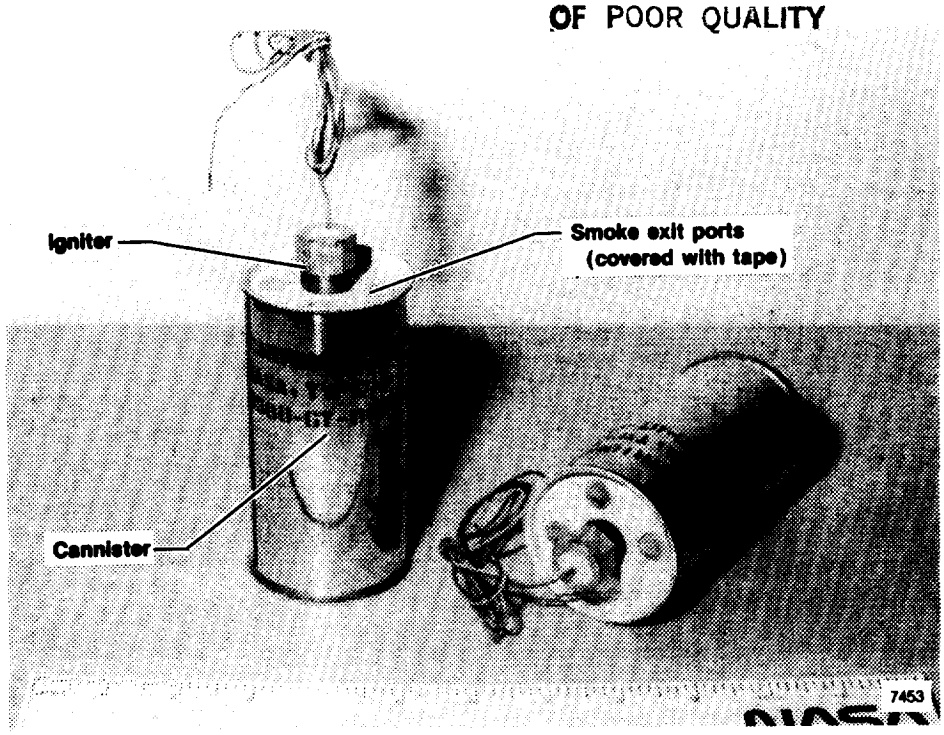

EC88-0069-009

Figure 20. F-18 HARV smoke cartridges.

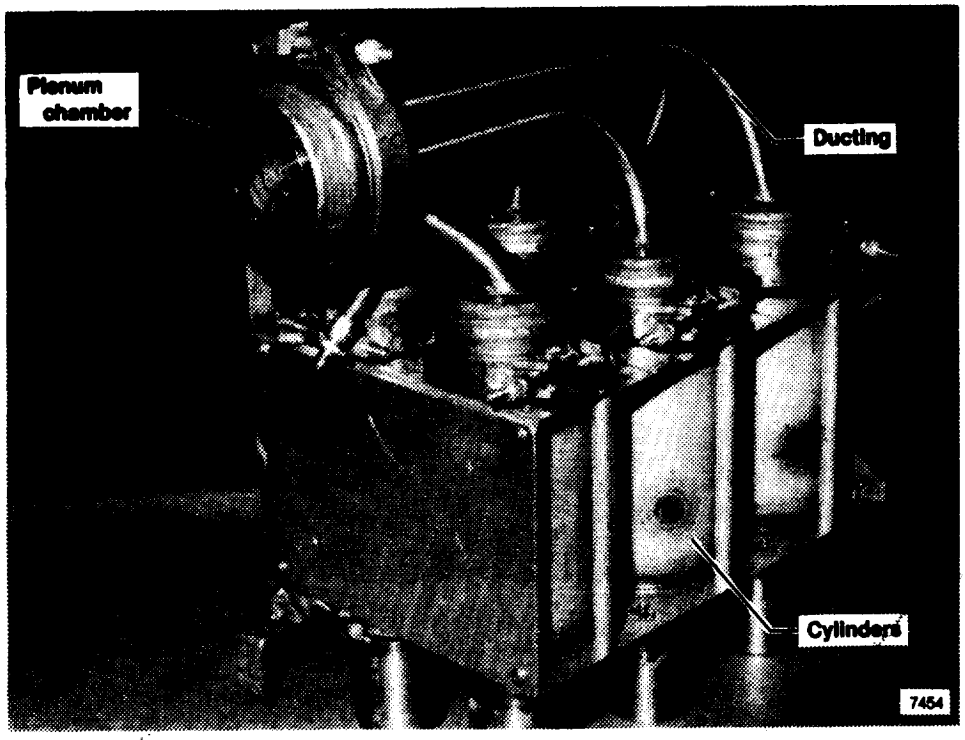

C86-33597-005

Figure 21. F-18 HARV smoke generator system (heater blanket removed).

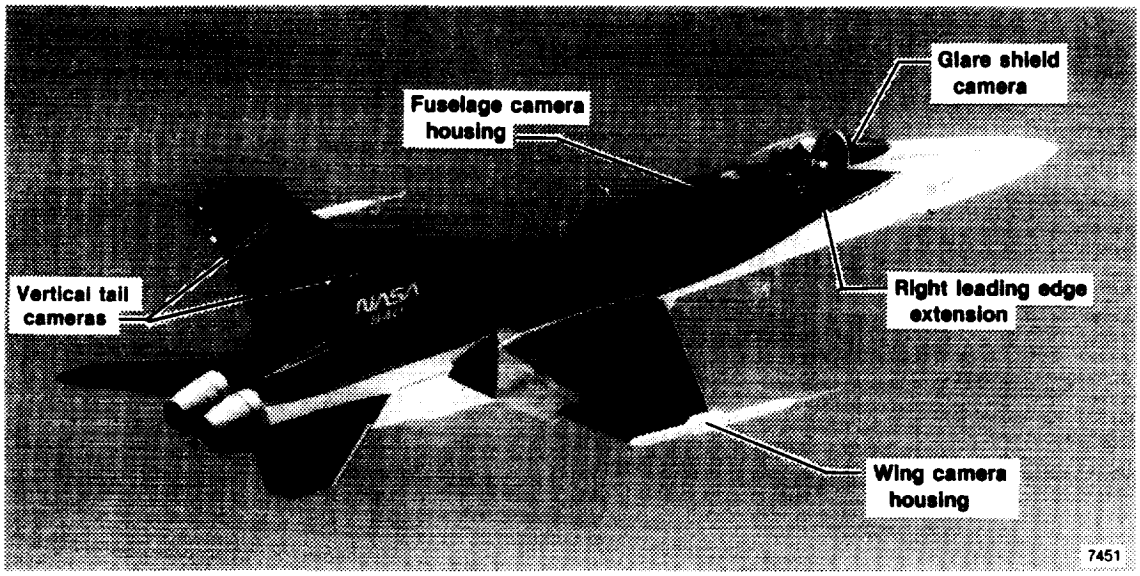

EC88-0095-003

Figure 22. F-18 HARV showing location of cameras.

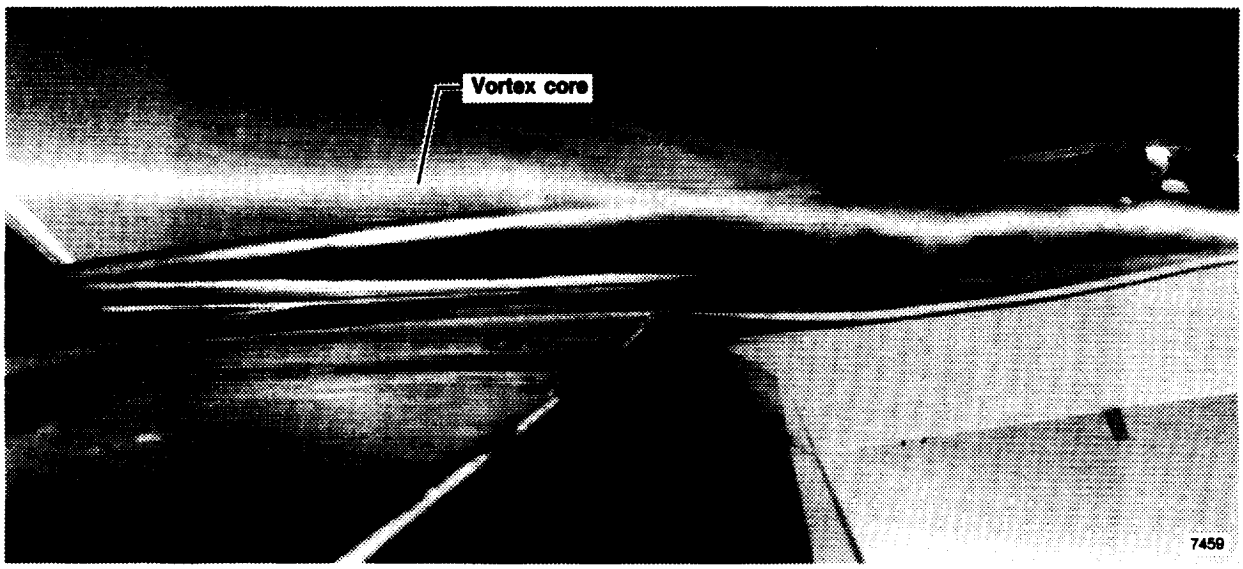

EC88-0094-010

(a) 15.0° angle of attack.

Figure 23. Examples of in-flight flow visualization with smoke generator system on F-18 HARV, view from wingtip camera.

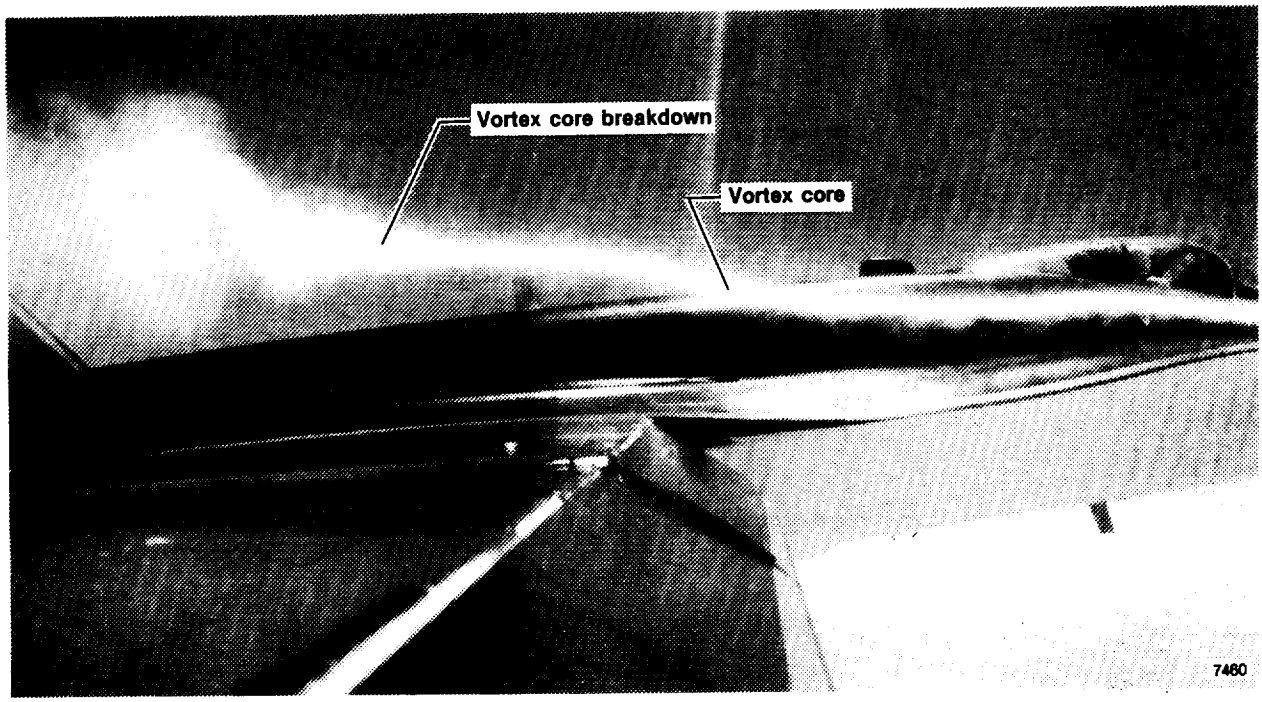

EC88-0094-032

(b) 20.8° angle of attack.

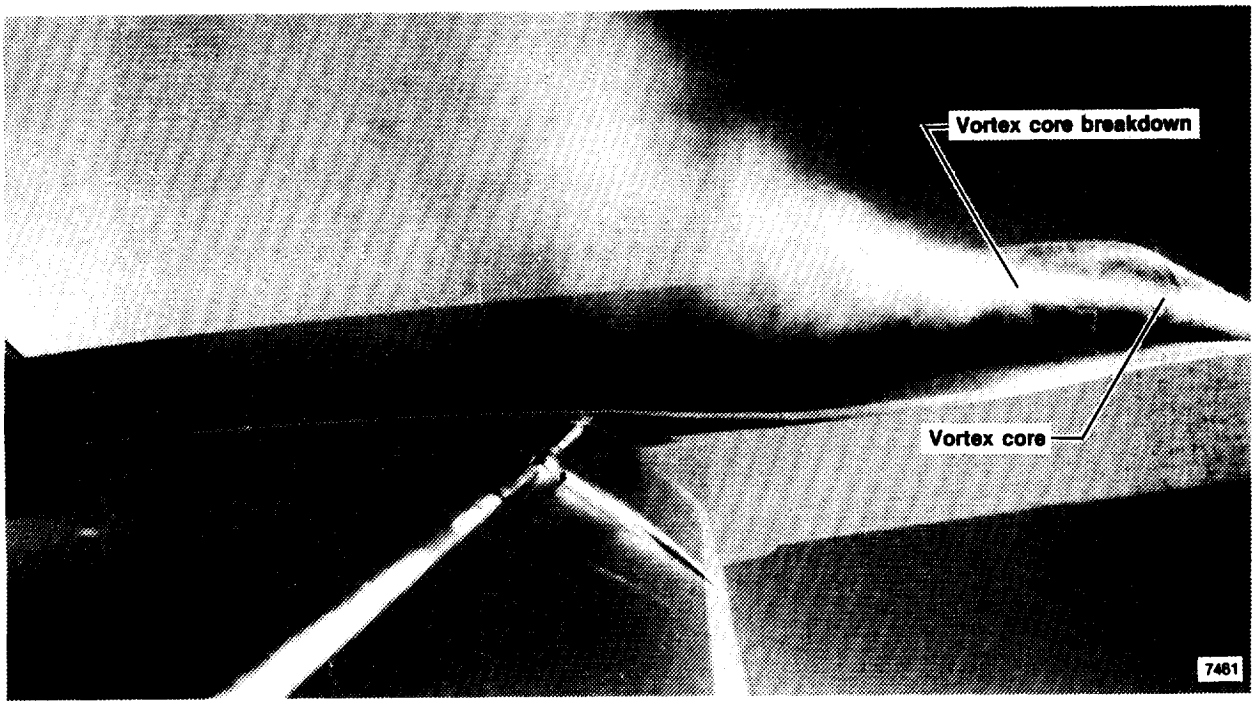

EC88-0094-026

(c) 34.6° angle of attack.

Figure 23. Concluded.

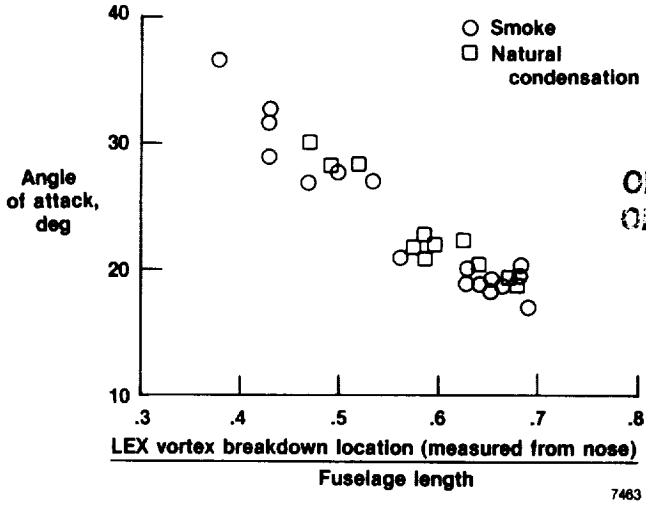

Figure 24. LEX vortex breakdown location variation with angle of attack.

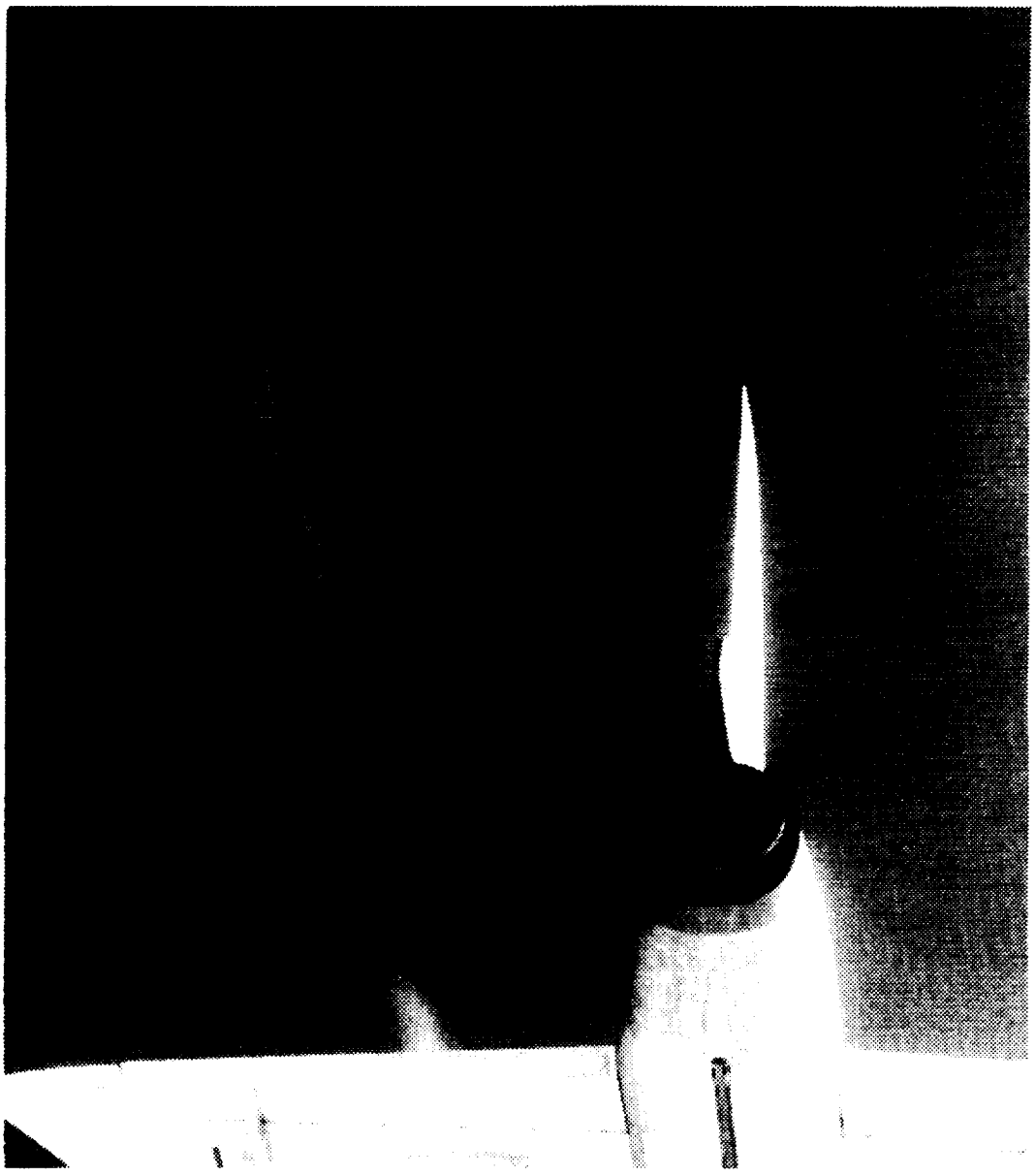

Figure 25. Persistence of propylene glycol smoke from F-106B aircraft.

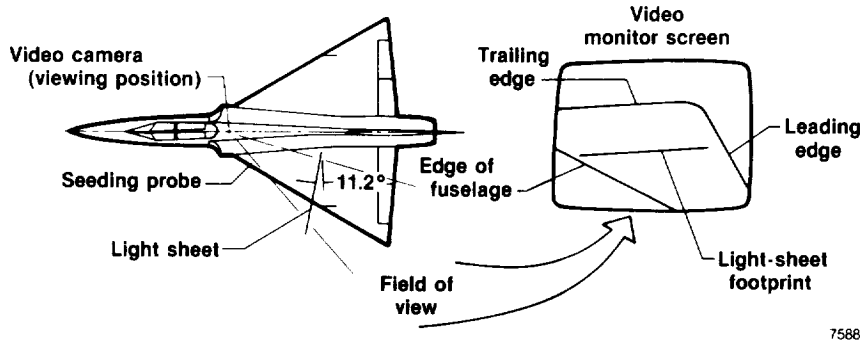

Figure 26. In-flight leading-edge-vortex flow visualization system on F-106B aircraft.

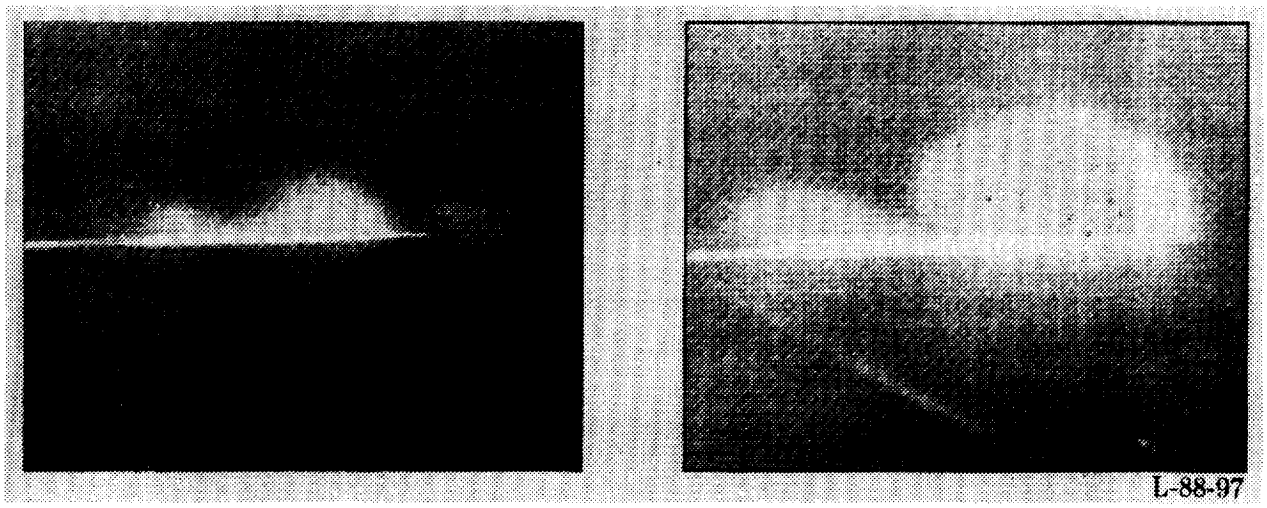

(a) Without digital enhancement.

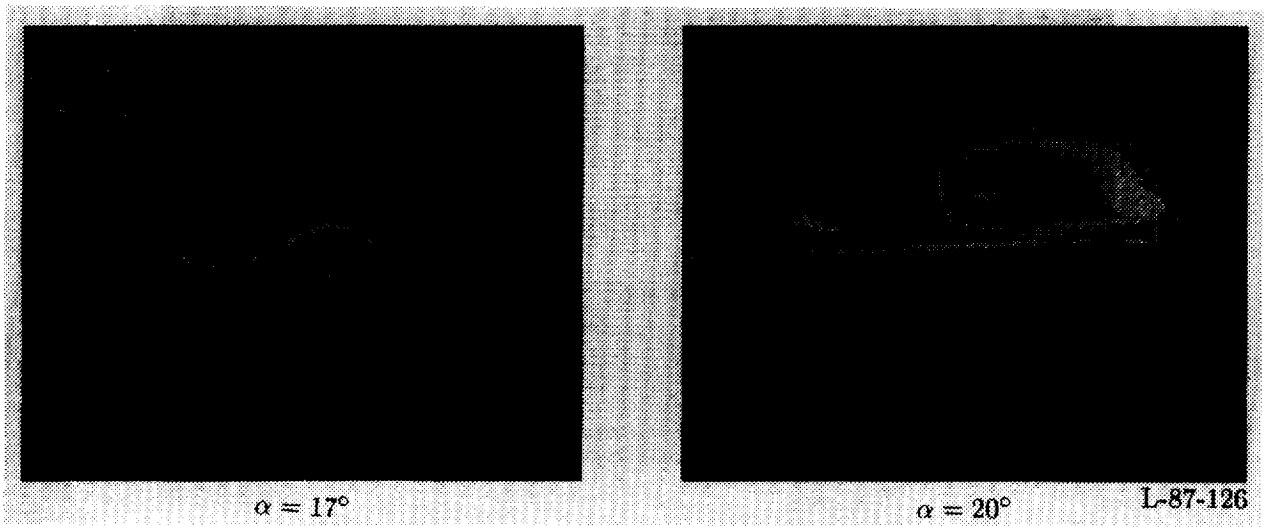

(b) With digital enhancement.

Figure 27. Vapor-screen images without and with digital enhancement from F-106B aircraft. $M_\infty = 0.4$, $R_n = 30 \times 10^6$, $h_p = 25{,}000$ ft, 1-g maneuver.

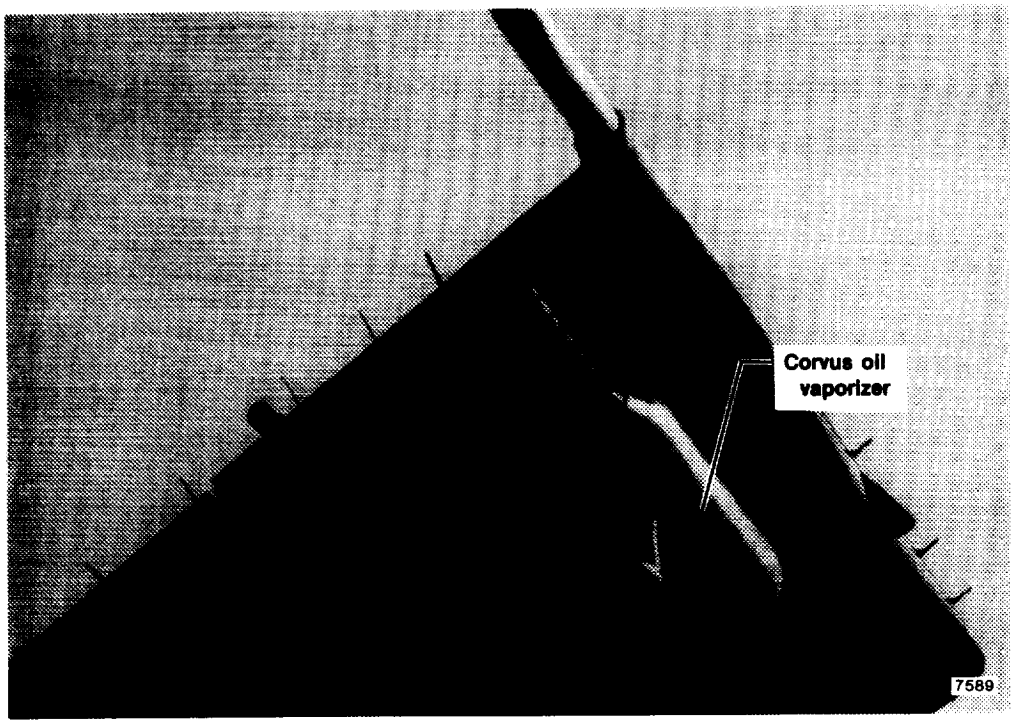

E-27819

Figure 28. Corvus oil vaporizer mounted on B-747 aircraft wing.

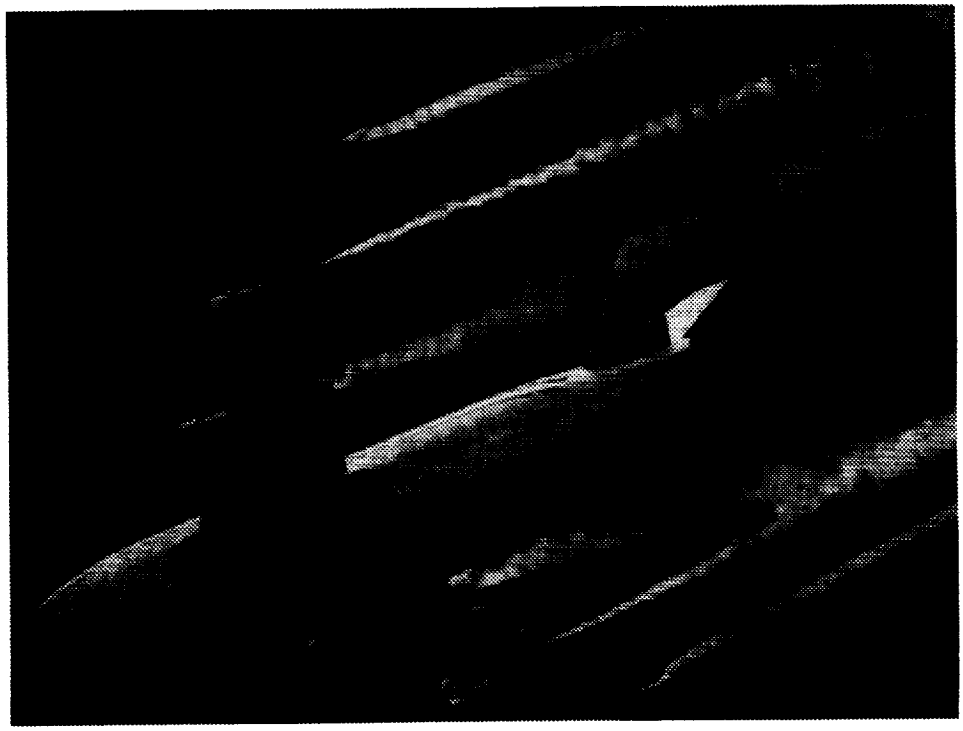

ECN 4240

Figure 29. B-747 aircraft wake vortex patterns using corvus oil vaporizers.

NASA
National Aeronautics and Space Administration

Report Documentation Page

1. Report No.	2. Government Accession No.	3. Recipient's Catalog No.
NASA TM-100455		

4. Title and Subtitle	5. Report Date
Flow Visualization Techniques for Flight Research	October 1988
	6. Performing Organization Code

7. Author(s)	8. Performing Organization Report No.
David F. Fisher and Robert R. Meyer, Jr.	H-1524
	10. Work Unit No.
	RTOP 505-68-71

9. Performing Organization Name and Address	11. Contract or Grant No.
NASA Ames Research Center Dryden Flight Research Facility P.O. Box 273, Edwards, CA 93523-5000	
	13. Type of Report and Period Covered
12. Sponsoring Agency Name and Address	Technical Memorandum
National Aeronautics and Space Administration Washington, DC 20546	14. Sponsoring Agency Code

15. Supplementary Notes

Presented as paper number 20 at the 73rd AGARD Symposium of the Flight Mechanics Panel on Flight Test Techniques, October 17–20, 1988, Edwards Air Force Base, California.

16. Abstract

In-flight flow visualization techniques used at the Dryden Flight Research Facility of NASA Ames Research Center (Ames-Dryden) and its predecessor organizations are described. Results from flight tests which visualized surface flows using flow cones, tufts, oil flows, liquid crystals, sublimating chemicals, and emitted fluids have been obtained. Off-surface flow visualization of vortical flow has been obtained from natural condensation and two methods using smoke generator systems. Recent results from flight tests at NASA Langley Research Center using a propylene glycol smoker and an infrared imager are also included. Results from photo-chase aircraft, onboard and postflight photography are presented.

17. Key Words (Suggested by Author(s))	18. Distribution Statement
Boundary layer transition Flight testing Flow visualization Vortex flow	Unclassified — Unlimited Subject category 02

19. Security Classif. (of this report)	20. Security Classif. (of this page)	21. No. of pages	22. Price
Unclassified	Unclassified	35	A03

NASA FORM 1626 OCT 86

**For sale by the National Technical Information Service, Springfield, VA 22161-2171.*